

Hadrons in the Nuclear Medium

M M Sargsian¹, J Arrington², W Bertozzi², W Boeglin¹,
 C E Carlson⁴, D B Day⁵, L L Frankfurt⁶, K Egiyan⁷, R Ent⁸,
 S Gilad², K Griffioen⁴, D W Higinbotham⁸, S Kuhn⁹,
 W Melnitchouk⁸, G A Miller¹⁰, E Piasetzky⁶, S Stepanyan^{8,9},
 M I Strikman¹¹ and L B Weinstein⁹

¹ Florida International University, University Park, FL, USA

² Argonne National Laboratory, Argonne, IL, USA

³ Massachusetts Institute of Technology, Cambridge, MA, USA

⁴ College of William and Mary, Williamsburg, VA, USA

⁵ University of Virginia, Charlottesville, VA, USA

⁶ Tel Aviv University, Tel Aviv, Israel

⁷ Yerevan Physics Institute, Yerevan, Armenia

⁸ Thomas Jefferson National Accelerator Facility, Newport News, VA, USA

⁹ Old Dominion University, Norfolk, VA, USA

¹⁰ University of Washington, Seattle, WA, USA

¹¹ Pennsylvania State University, University Park, PA, USA

Abstract. Quantum Chromodynamics, the microscopic theory of strong interactions, has not yet been applied to the calculation of nuclear wave functions. However, it certainly provokes a number of specific questions and suggests the existence of novel phenomena in nuclear physics which are not part of the traditional framework of the meson-nucleon description of nuclei. Many of these phenomena are related to high nuclear densities and the role of color in nucleonic interactions. Quantum fluctuations in the spatial separation between nucleons may lead to local high density configurations of cold nuclear matter in nuclei, up to four times larger than typical nuclear densities. We argue here that experiments utilizing the higher energies available upon completion of the Jefferson Laboratory energy upgrade will be able to probe the quark-gluon structure of such high density configurations and therefore elucidate the fundamental nature of nuclear matter. We review three key experimental programs: quasi-elastic electro-disintegration of light nuclei, deep inelastic scattering from nuclei at $x > 1$, and the measurement of tagged structure functions. These interrelated programs are all aimed at the exploration of the quark structure of high density nuclear configurations.

The study of the QCD dynamics of elementary hard processes is another important research direction and nuclei provide a unique avenue to explore these dynamics. In particular, we argue that the use of nuclear targets and large values of momentum transfer at energies available with the Jefferson Laboratory upgrade would allow us to determine whether the physics of the nucleon form factors is dominated by spatially small configurations of three quarks. Similarly, one could determine if hard two-body processes such as exclusive vector meson electroproduction are dominated by production of mesons in small-size $q\bar{q}$ configurations.

1. Open questions in our understanding of nuclear structure

Quantum Chromodynamics (QCD), the only legitimate candidate for a theory of strong interactions, is a non-Abelian gauge theory with gauge group $SU(3)$ (in color space) coupled to quarks in the fundamental (triplet) representation. It contains the remarkable postulate of exact $SU(3)$ color symmetry. Quarks and gluons carry color and are the fundamental particles that interact via the color force. An important feature of this theory is that the u and d quarks, for the purpose of the strong interaction, are regarded as massless. In this limit, chiral symmetry is spontaneously broken in the ground state of QCD.

Nuclei should provide an excellent testing ground for this theory because nuclei are stable systems, made up of quarks and gluons bound together by the strong force. However, the quarks and gluons are hidden and nuclei seem to be composed of hadrons bound together by the exchange of evanescent mesons. The hadrons that are the constituents of nuclei are identified with color singlet states and have strong interactions very different in nature than that of gluon exchange by colored quarks and gluons.

There seems at first glance to be a contradiction between the fundamental theory, QCD, and the very nature of nuclei. This contradiction can be resolved by accounting for the fact that effective theories of the strong interaction, in which the degrees of freedom are hadrons, can yield results that are equivalent, over some range of kinematic resolution, to those of QCD. Indeed, it is widely realized that the phenomenon of the spontaneously broken chiral symmetry in QCD is equivalent to the pseudovector pion-nucleon interaction, which accounts for the long-range, low momentum transfer, aspects of nuclear physics. The same chiral structure also accounts for the relatively weak soft pionic fields in nuclei. Furthermore, at low momentum transfer the relevant degrees of freedom are quasi-particle excitations of the system described by Landau-Fermi liquid theory. Thus, while QCD is the fundamental theory of strong interactions, it is not required to explain the structure of nuclei observed in low-energy processes.

The availability of high energy beams provides the opportunity to observe features of nuclear structure at small distance scales, which may reveal the presence of QCD as the ultimate source of the strong interaction. The central features of QCD, quarks and color, lead to two separate, but related, avenues of experimental investigation which we examine in this review.

The first avenue is that of high density nuclear matter. What happens during the brief intervals when two or more nucleons overlap in space? Can we account for the interactions using meson exchanges, or do we instead need to consider explicitly quark aspects such as quark exchanges between nucleons and the kneading of the nucleon's constituents into six- or nine-quark bags? At high densities, can we detect the presence of superfast quarks, i.e. quarks carrying a light cone momentum fraction greater than that of a nucleon at rest?

The second avenue is concerned with the role of color in high momentum transfer processes which are exclusive (or sufficiently exclusive) so that the interference effects

of quantum mechanics must be taken into account. Then, the use of high momentum kinematics offers a remarkable opportunity to observe the color-singlet fluctuations of a hadron in configurations of very small spatial extent, *viz.*, point-like configurations. If such configurations exist, they do not interact strongly because the effects of the emitted gluons cancel, just as the interaction of an electric dipole decreases with size of dipole due to the cancellation of the electromagnetic interactions. Such effects are called color-coherent phenomena and include the subject known as color transparency. Thus, we are concerned with studying the diverse subjects of high-density cold nuclear matter and color coherence.

While these subjects are connected by their importance in establishing QCD as the underlying theory of the strong interaction, they may also come together in the understanding of exotic phenomena in nature. Studies of the local high-density fluctuations are important to understanding the equation of state of cold, dense matter which is crucial in understanding the possibility of the transition of neutron stars to more dense states like “quark stars”, whose experimental existence was suggested recently [1]. The phenomenon of color transparency means that for a short period of time a nucleon can be in a spatially small configuration. In this configuration, the nucleon can tunnel through the potential barrier given by the repulsive core of the nucleon-nucleon (NN) interaction. This provides a possible mechanism for a phase transition to a new form of matter for a sufficiently dense nuclear system, such as in the core of neutron star.

The following is a brief outline of this review. The quark-gluon physics of high density fluctuations in nuclei is examined in Sec. 2, which begins with a brief discussion of the relevant history. The discovery of the nuclear EMC effect almost twenty years ago brought the subjects of quarks into nuclear physics with great impact. However, the specific causes of the modifications observed in nuclear structure functions have not yet been identified with certainty. Thus, the questions regarding quark dynamics of nuclei raised by that momentous discovery have not yet been answered. The various ideas invoked to explain this effect are reviewed. We then argue that an experimental program focused on discovering scaling in deep inelastic scattering at high values of Bjorken- x (>1.2) will reveal the nature of high-density fluctuations of cold nuclear matter. Further deep inelastic scattering measurements of backward going nucleons in coincidence with the outgoing electron offer the promise of finally determining the cause of the EMC effect. Section 3 is concerned with the role of color in nuclear physics. Electron scattering experiments at high momentum transfer in which one or two nucleons are knocked out, performed with sufficient precision to verify that no other particles are produced, could reveal the fundamental nature of color dynamics: that, for coherent processes, the effects of gluons emitted by a small color singlet object are canceled. In that case, the dynamical nature of the nucleon form factor at high momentum transfer will be revealed. Similarly motivated experiments in which a vector meson is produced in a coherent reaction with a deuteron target at large momentum transfers are also discussed. Section 4 presents a summary of the plan proposed to investigate the questions arising from the study of hadrons in the nuclear medium.

2. Quark-gluon Properties of Superdense Fluctuations of Nuclear Matter

2.1. A Brief History and Short Outlook

We begin this section with a brief discussion of the history of experimental lepton-nuclear physics. Prior to the completion of Thomas Jefferson National Accelerator Facility (Jefferson Lab), experimental studies of nuclei using lepton probes could be discussed in terms of two clearly different classes:

(a) Experiments performed at electron machines with low incident electron energies, $E_{inc} \leq 1$ GeV, in which the typical energy and momentum transfers, ν and \vec{q} , were comparable to the nuclear scale

$$\nu \leq 100 \text{ MeV}, |\vec{q}| \leq 2 k_F, \quad (1)$$

where $k_F \approx 250$ MeV/c is the characteristic Fermi momentum of nuclei. These reactions were inclusive (e, e') and semi-inclusive ($e, e'N$) and covered mainly the quasi-elastic and the low lying resonance regions (the Δ isobars), corresponding to relatively large values of Bjorken- x ($x = Q^2/2m_p\nu$, where $Q^2 = q^2 - \nu^2$).

(b) Deep inelastic scattering (DIS) experiments which probed nuclei at $x < 1$ and large Q^2 scales, greater than about 4 GeV², which resolved the parton constituents of the nucleus.

The first class of experiments are unable to resolve the short range structure of nuclei, and the second, while having good resolution, typically involved inclusive measurements which averaged out the fine details and were limited by low luminosities and other factors.

It is interesting to notice that there is a clear gap between the kinematic regions of these two classes of experiments. This corresponds exactly to the optimal range for the study of the nucleonic degrees of freedom in nuclei, $1.5 \leq Q^2 \leq 4$ GeV², for which short-range correlations (SRCs) between nucleons can be resolved, and the quark degrees of freedom are only a small correction. Work at Jefferson Lab has started to fill this gap in a series of quasi-elastic $A(e, e')$, $A(e, e'N)$, and $A(e, e'N_1N_2)$ experiments. Previously, this range was just touched by inclusive experiments at SLAC[2, 3, 4, 5] which also provided the first measurement of $A = 2, 3, 4$ form factors at large Q^2 . A number of these high-energy experiments probe the light-cone projection of the nuclear wave function and in particular the light-cone nuclear density matrix, $\rho_A^N(\alpha, p_\perp)$, in the kinematics where the light-cone momentum fraction $\alpha \geq 1$ ($A \geq \alpha \geq 0$) so that short range correlations between nucleons play an important role.

It is already known that the existence of SRCs gives a natural explanation of the practically A -independent spectrum of the emission of fast backward nucleons and mesons, as well as the practically Q^2 - and x -independent value of the ratio of $\sigma_A(x, Q^2)/\sigma_{D(^3He)}(x, Q^2)$ for $Q^2 \geq 1$ GeV² and $1.5 \leq x \leq 2$ [6, 7, 8]. Overall, these and other high-energy data indicate a significant probability of these correlations ($\sim 25\%$ of nucleons in heavy nuclei) which involve momenta larger than the Fermi momentum. These probabilities are in qualitative agreement with calculations of nuclear wave

functions using realistic NN potentials [9]. Most of this probability ($\sim 80\%$) is related to two-nucleon SRCs with the rest involving $N \geq 3$ correlations (see e.g., Ref. [10]). The current experiments at Jefferson Lab will allow a detailed study of two-nucleon SRCs [11, 12], and take a first look at three-nucleon correlations [12, 13]. We expect that experiments at an electron energy of up to 11 GeV [14] will allow further explorations of SRCs in the three-nucleon correlation region, substantially extending the region of initial nucleon momenta and the recoil nucleus excitation energies that can be probed in quasi-elastic $A(e, e')$, $A(e, e'N)$, and $A(e, e'N_1N_2)$ reactions.

The 12 GeV upgrade at Jefferson Lab[‡] will also be of a great benefit for studies of deep inelastic scattering off nuclei (experiments in class (b)). It will enable us to extend the high Q^2 inclusive $A(e, e')$ measurement at $x \geq 1$ to the deep inelastic region where the process is dominated by the scattering from individual quarks in the nucleus with momenta exceeding the average momentum of a nucleon in the nucleus (superfast quarks). Such quarks are likely to originate from configurations in which two or more nucleons come close together. Thus, these measurements will complement the studies of SRCs by exploring their sub-nucleonic structure.

The second extension of class (b) reactions concerns the measurement of nuclear DIS reactions in the $(e, e'N)$ semi-inclusive regime, in which the detection of the additional nucleon in spectator kinematics will allow us to tag electron scattering from a bound nucleon. These studies may provide a number of unexpected results similar to those in the inclusive studies of parton densities in nuclei, which yielded the observation of the EMC effect [15, 16, 17]: a depletion of the nuclear quark parton density as compared to that in a free nucleon at $0.4 \leq x \leq 0.8$, which demonstrated unambiguously that nuclei cannot be described merely as a collection of nucleons without any extra constituents.

Among several suggested interpretations of the EMC effect, the idea of mesonic degrees of freedom (nuclear binding models) was the only one which produced a natural link to the meson theory of nuclear forces. This explanation naturally led to a prediction of a large enhancement of the anti-quark distribution in nuclei [18, 19, 20]. A dedicated experiment was performed at Fermi Lab using the Drell-Yan process to measure the ratio $R_A^{\bar{q}}(x, Q^2) \equiv \frac{\bar{q}_A(x, Q^2)}{Aq_N(x, Q^2)}$. The result of this experiment [21] was another major surprise: instead of a $\sim 10 - 20\%$ enhancement of $R_A^{\bar{q}}(x, Q^2)$, a few percent suppression was observed. Further indications of the unexpected partonic structure of nuclei come from the studies of the gluon densities in nuclei using exact QCD sum rules [22, 23] as well as the analysis [24] of the data on the scaling violation of $R_A^q(x, Q^2)$ indicate that the gluon densities should be significantly enhanced in nuclei at $x \sim 0.1$. However the inclusive nature of these measurements does not provide insight into the QCD mechanism for the depletion of the DIS structure functions. The semi-inclusive DIS $(e, e'N)$ reactions with the detection of backward-going nucleons will test many models of the EMC effect, which was previously impossible due to the inclusive nature of (e, e') reactions. Semi-inclusive DIS reactions are ultimately related to the understanding of the QCD dynamics

[‡] The energy upgrade planned for Jefferson Lab will provide 11 GeV electrons to the experimental Halls A, B, and C, see [14].

of multi-nucleon systems at small distances. Thus, it is crucial that these studies be done in parallel with the above mentioned studies of SRCs.

2.2. The Big Picture of Small Distance Fluctuations

The proton electromagnetic radius is ~ 0.86 fm, and in the ground state of infinite nuclear matter the average (center-to-center) distance between nearby nucleons is ~ 1.7 fm. Thus, under normal conditions nucleons are closely packed and nearly overlap. Despite this, quark aspects of nuclear structure are not evident for most of nuclear physics. A possible dynamical explanation for this, in terms of the strong-coupling limit of QCD, was presented in Ref. [25]. This can also be seen from the fact that typical nuclear excitations are at much lower energies than nucleon excitations ($\gtrsim 500$ MeV). Besides, in low energy QCD, the pion, being a pseudogoldstone, interacts with the amplitude $\propto k_\pi$, leading to a suppression of the near-threshold pion (multi-pion) production.

However, quantum fluctuations must occur in any quantum system, and well-designed experiments may expose the physics occurring when nucleons occasionally encounter each other at smaller than average distances. If such a fluctuation reduces the center-to-center separation to 1 fm, then there is a significant region of overlap. Assuming a uniform nucleon charge distribution, the density in the region of overlap is twice that of the nucleon, or about four to five times that of normal nuclear matter, $\rho_0 = 0.17$ nucleon/fm³. At these densities, the physics of confinement, which typifies the strong-coupling limit of QCD, may no longer be applicable and the chiral symmetry may be (partially) restored, see e.g. [26]. One can also think of these high-density fluctuations as nuclear states with excitation energies large enough to modify the structure of underlying nucleonic constituents. Hence, dense nuclear matter may look very different from a system of closely packed nucleons. From this viewpoint, it is encouraging that experimental data on the EMC effect indicate that deviations from the expectations of the nucleonic model of nuclei grow approximately linearly with the nuclear density, suggesting that the properties of the quark-gluon droplets could indeed deviate very strongly from those of a collection of nucleons.

It is important to recall that the properties of dense nuclear matter are closely related to outstanding issues of QCD such as the existence of chiral symmetry restoration and deconfinement, as well as determining the nature of the onset of quark-gluon degrees of freedom and the structure of the phase transition from hadronic to quark-gluon states of matter. In QCD, transitions to new phases of matter are possible in different regimes of density and temperature. In particular, it has been suggested [27] that nuclear matter could exist in a color superconductivity phase caused by the condensation of diquarks. Recent estimates suggest that the average nuclear density could lie in between that of the dilute nucleon phase and the superconducting phase [28, 29]. It is therefore natural to ask whether one can observe precursors of such a phase transition by studying the quark-gluon properties of superdense droplets of nuclear matter, i.e., configurations when two

or more nucleons come close together. It should also be remembered that the EMC effect has been interpreted as a delocalization of quarks in nuclei, which is qualitatively consistent with a proximity to the phase transition. More recently, measurements of in-medium proton form factors also hint at such a modification of nucleon structure [30].

So far, the major thrust of studies looking for the phase transitions in hadronic matter has been focused in the high temperature region (Fig. 1), which may be realized in high-energy heavy-ion collisions. The low temperature region of high densities, critical for building the complete picture of phase transitions and for determining if the transition from neutron to quark stars is possible, is practically unexplored. We wish to argue that this unexplored low temperature region, crucial for the understanding of the equation of state of neutron stars, is amenable to studies using high energy lepton probes. Jefferson Lab, upgraded to higher energies [14], would be able to explore this region and provide studies of nuclear fluctuations as dense as $4\text{--}5 \rho_0$.

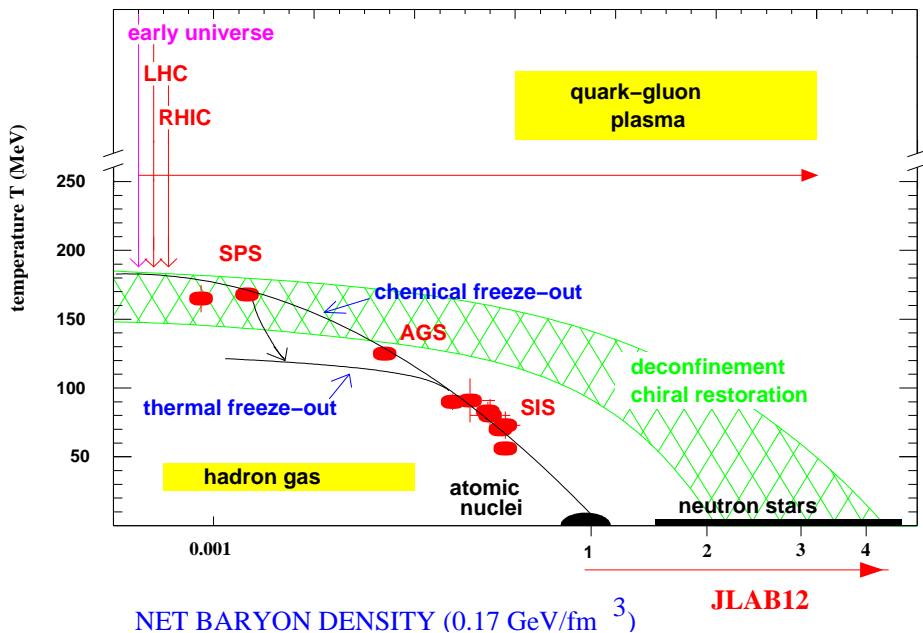


Figure 1. Phase diagram for baryonic matter.

2.3. Outline of the experimental program

The intellectual problems associated with establishing the existence of high density fluctuations of nuclear matter are formidable. We cannot conceive of a single experiment which would be able to answer all of the interesting questions about the role of non-nucleonic degrees of freedom, but a series of correlated measurements may succeed. As mentioned above, we anticipate that studies to be done at Jefferson Lab at 6 GeV will provide additional information about nucleonic degrees of freedom in the $2N$ sector of SRCs. This will certainly help us in refining the envisioned experimental program.

Our view is that three key experimental programs, for which the use of 12 GeV electrons is essential, are needed.

- Quasi-elastic electro-disintegration of light nuclei at $1.5 \leq Q^2 \leq 4 \text{ GeV}^2$, covering a wide range of angles and missing momenta \S (in excess of 1 GeV/c), with the goal of probing the structure of SRCs.
- Deep inelastic scattering at $x > 1$, with the goal of observing superfast quarks in nuclei.
- Tagged structure functions (measurement of a nucleon from the target fragmentation region in coincidence with the outgoing electron) with the goal of directly observing the presence of non-nucleonic degrees of freedom in droplets of superdense matter.

The first goal of studying SRCs using quasi-elastic electro-disintegration of light nuclei is based on the capabilities of Jefferson Lab to perform fully exclusive measurements. The exclusive reactions using a deuteron target in a wide range of recoil nucleon momenta and angles will allow us to obtain insight into many fundamental questions, e.g. the probability of pre-existing non-nucleon components in the deuteron wave function, the transition of meson currents to the quark-interchange mechanism in the NN interaction, and the dynamical structure of the nuclear core. For heavier ($A = 3, 4$) nuclei, the capability to measure a recoil nucleon with light cone momentum fraction $\alpha \geq 2$ will provide direct access to the three-nucleon correlation structure of the nuclear wave function providing the unprecedented opportunity to study the dynamics of the three-nucleon force.

The second goal of learning about superfast quarks will be accomplished by studying inclusive electron nucleus scattering in the scaling region at $x \geq 1$, where this process measures, *in a model independent way*, the probability of finding a quark that carries a larger light-cone momentum than one would expect from a quark in a low-momentum nucleon ($k \leq k_F$). Obviously, very few such superfast quarks can originate from the effects of the nuclear mean field, but the uncertainty principle indicates that such quarks in nuclei could arise from fluctuations of superdense configurations consisting either of a few overlapping nucleons with large momenta, or of more complicated multi-quark configurations. The study of the structure of these superdense fluctuations would be the major goal of deep inelastic scattering measurements at high x . For instance, high precision measurements of the A -dependence of the cross section would permit the investigation of the density dependence of the superfast quark probability in the nuclear medium. The functional dependence of this probability on Bjorken- x would allow us to disentangle the contributions of two- or multi-nucleon droplets from more exotic components (e.g., 6-, or 9-quark bags).

The third goal of determining the modification of the quark-gluon structure of nucleons in a dense nuclear environment could be realized by measuring tagged structure

\S We define the missing momentum as the difference between momenta of knocked-out nucleon and virtual photon.

functions in semi-inclusive DIS reactions. For example, the observation of a backward-moving nucleon or nucleons will be used as a tag to select hard scattering from a short-range correlation of nucleons while the DIS characteristics of the event will be used to study modifications of the parton density. These studies primarily require the isolation of a backward-moving nucleon for which a tagging procedure, rather than reconstruction of a missing nucleon, will provide the cleanest signature.

Successful completion of these programs will allow significant progress in understanding such unresolved topics of strong interaction physics as, *interaction of quarks at high densities and low temperatures*, and *the quark-gluon structure of nuclei*.

2.4. Nucleonic Structure of Short-Range Correlations

The first step of the program will be to study the structure of SRCs in terms of nucleonic degrees of freedom, and map out the strength of two-nucleon and multi-nucleon correlations in nuclei. This can be accomplished by combining moderate energy (4–6 GeV) inclusive scattering experiments from light and heavy nuclei with moderate and higher energy coincidence reactions on few-body nuclei, as described in the previous section. Here we present an experimental overview of these reactions.

2.4.1. Qualitative Features of High- Q^2 Electro-Nuclear Reactions The observation of SRCs in nuclei has long been considered one of the most significant aims of nuclear physics. These correlations, though elusive, are not small: calculations of nuclear wave functions with realistic NN potentials consistently indicate that in heavy nuclei about 25% of the nucleons have momenta above the Fermi surface [9]. This corresponds to about 50% of the kinetic energy coming from SRCs. The problem has been a lack of experimental data at high-momentum transfer kinematics which could decisively discriminate between the effects of the SRCs in the initial state and the long-range multi-step effects such as final state interactions (FSIs) and meson exchange currents (MECs). Before we can proceed to study SRCs in nuclei, we must consider these processes. In the following sections, we will show that some of these effects are suppressed at high Q^2 , while the remaining effects do not mask the dynamics of the SRCs.

Final State Interactions:

Although final state interactions in nucleon knockout reactions do not disappear at large Q^2 , two important simplifications occur which make the extraction of information about the short-range nuclear structure possible:

- In high energy kinematics a new (approximate) conservation law exists - the light-cone momentum fractions of slow nucleons do not change if they scatter elastically with the ejected nucleon which maintains its high momentum during the rescattering [31, 32].

To demonstrate this feature let us consider the propagation of a fast nucleon with four-momentum $k_1 = (\epsilon_1, 0, k_{1z})$ through the nuclear medium. We chose the z -axis

in the direction of \mathbf{k}_1 such that $\frac{k_{1-}}{m} \equiv \frac{\epsilon_1 - k_{1z}}{m} \approx \frac{m}{2k_{1z}} \ll 1$. After this nucleon makes a small angle rescattering in its interaction with a bound nucleon of four-momentum $p_1 = (E_1, p_{1\perp}, p_{1z})$, it maintains its high momentum and leading z -direction with the four-momentum $k_2 = (\epsilon_2, k_{2\perp}, k_{2z})$, where $\frac{k_{2\perp}^2}{m_N^2} \ll 1$. The bound nucleon four-momentum becomes $p_2 = (E_2, p_{2\perp}, p_{2z})$. The energy momentum conservation for this scattering allows us to write for the “-” component ($p_- = E - p_z$):

$$k_{1-} + p_{1-} = k_{2-} + p_{2-}. \quad (2)$$

From Eq.(2) for the change of the “-” component of the bound nucleon momentum one obtains

$$\frac{\Delta p_-}{m} \equiv \frac{p_{2-} - p_{1-}}{m} \equiv \alpha_2 - \alpha_1 = \frac{k_{1-} - k_{2-}}{m} \ll 1, \quad (3)$$

where we define $\alpha_i = \frac{p_{i-}}{m}$ ($i = 1, 2$) and use the fact that $\frac{k_{2\perp}^2}{m_N^2}, \frac{k_{1\perp}^2}{m_N^2} \ll 1$. Therefore $\alpha_1 \approx \alpha_2$. The latter indicates that, with an increase of energy, a new conservation law emerges in which the light-cone momentum fractions of slow nucleons, α , are conserved. The unique simplification of the high energy rescattering is that although both the energy and momentum of the bound nucleon are distorted due to rescattering, the combination $E - p_z$ is not.

Figure 2 demonstrates the accuracy of this conservation law for a propagating nucleon over a range of four-momenta relevant to our discussion. It is important to note that the average transferred momentum in the NN rescattering amplitude for $p_N \sim 3 - 10$ GeV/c is $\langle k_t^2 \rangle \approx 0.25$ (GeV/c)². Thus, starting from 3 GeV/c momenta of the propagating nucleon, the conservation of α ($\sim \mathcal{O}(1)$) is accurate to better than 5% and improves with increasing momentum. Note that the conservation of α to this level is sufficient for studying SRCs for which the α distribution of the nucleons has a rather slow, ($\propto \exp(-\lambda\alpha), \lambda \sim 7$) variation. Indeed, this variation is expected to be much flatter than the corresponding distribution generated by a mean-field interaction.

- The small angle scatterings of high-energy ($2 \leq p_N \leq 10$ GeV/c) nucleons can be described by the generalized eikonal approximation (GEA) which takes into account the difference between the space-time picture of the proton-nucleus scattering (a proton coming from $-\infty$) and $A(e, e'p)$ process (a proton is produced inside the nucleus), and also accounts for the non-zero Fermi momenta of rescattered nucleons [31, 32]. Additionally, the description of small angle rescattering is simplified due to approximate energy independence of the pp and pn total cross sections in the high Q^2 limit (starting at $Q^2 \geq 2$ GeV², which corresponds to $p_N \geq 2$ GeV/c).

The above two features of small angle rescattering in the high Q^2 domain make it possible to evaluate FSIs reliably, identifying kinematic requirements which will allow us to separate SRC effects from long range FSI contributions.

Note that the minimal value of Q^2 for which one expects the eikonal approximation to be valid can be estimated from the application of Glauber theory to pA reactions.

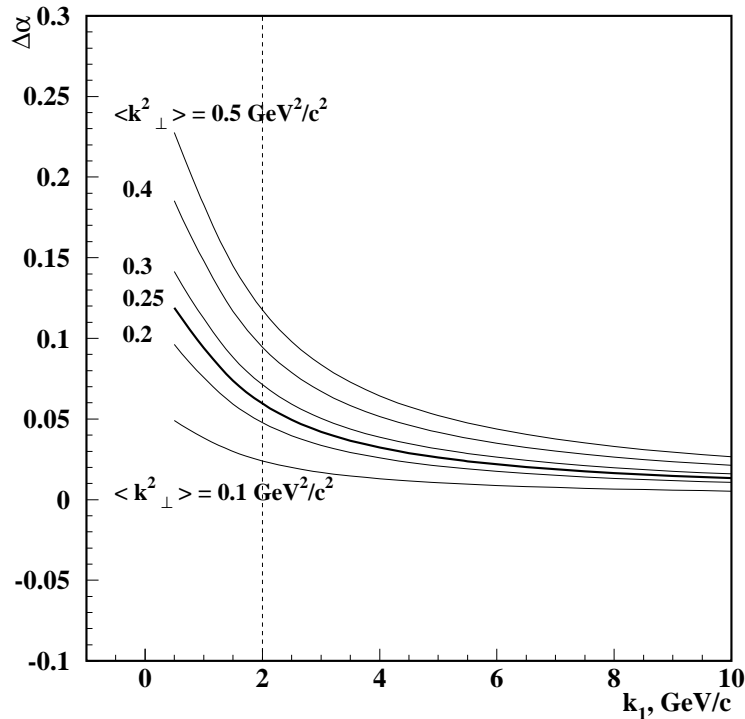


Figure 2. The accuracy of the conservation of α as a function of the propagating nucleon momentum, k_1 at different values of average transferred (during the rescattering) momenta, $\langle k_{\perp}^2 \rangle$. Note that the eikonal approximation is theoretically justified for $k_1 \geq 2$ GeV/c.

Extensive studies have demonstrated long ago that the Glauber theory of pA processes can describe the data within a few percent starting at energies as low as $E_p^{inc} \geq 0.8 - 1$ GeV, which corresponds to $Q^2 \geq 1.5$ GeV² in $(e, e'N)$ and $(e, e'N_1N_2)$ reactions.

Contribution of Meson Exchange Currents:

The major problem we face in the estimation of MECs in $A(e, e'N)$ processes is that with an increase of energies the virtuality of the exchanged mesons grows proportional to Q^2 ($\gg m_{meson}^2$). Even though the idea of deeply virtual exchanged mesons is highly complicated or may even be meaningless (see discussion in Ref. [33]), one can still estimate its Q^2 -dependence as compared to the SRC contribution.

In a kinematic setting typical for studies of SRCs, in which the knocked-out nucleon carries almost the entire momentum of the virtual photon (while the missing four-momentum of the recoil system does not change with Q^2), the Q^2 -dependence of the MEC amplitude can be estimated as follows:

$$\begin{aligned}
 A_{MEC}^{\mu} &\sim \int d^3p \cdot \Psi(p) \frac{J_m^{\mu}(Q^2)}{(Q^2 + m_{meson}^2)} \Gamma_{MNN}(Q^2) \\
 &\propto \int d^3p \cdot \Psi(p) \left(\frac{1}{(Q^2 + m_{meson}^2)^2 (1 + Q^2/\Lambda^2)^2} \right), \quad (4)
 \end{aligned}$$

where $J_m^\mu(Q^2)$ is the meson electromagnetic current proportional to the elastic form factor of the meson $\sim \frac{1}{Q^2 + m_{\text{meson}}^2}$, and $m_{\text{meson}}^2 \approx 0.71 \text{ GeV}^2$. For the meson-nucleon vertices, $\Gamma_{MNN}(Q^2)$, we assume a dipole dependence with $\Lambda \sim 0.8 - 1 \text{ GeV}^2$.

Since the leading Q^2 -dependence in the SRC contribution comes from the nucleon elastic form factors, Eqn. (4) will result in an additional $\sim (1 + Q^2/\Lambda^2)^{-2}$ suppression of the MEC amplitude as compared to the SRC contribution. Note that this gives an upper limit to the MEC contribution, since for large Q^2 the quark counting rule predicts stronger Q^2 suppression for $\Gamma_{MNN}(Q^2) \sim \frac{1}{Q^6}$ [34]. Thus, one expects that MEC contributions will be strongly suppressed as soon as Q^2 is greater than m_{meson}^2 and Λ^2 , both $\sim 1 \text{ GeV}^2$. This conclusion is relevant only for small angle nucleon knock-out kinematics (optimal for studies of SRCs). In the large angle kinematics quark-exchange mechanism may become important similar to the large angle $\gamma d \rightarrow pn$ reactions[35].

Isobar Current (IC) Contribution:

For the case of IC contributions, the virtual photon produces the Δ isobar in the intermediate state which subsequently rescatters off the spectator nucleon through the $\Delta N \rightarrow NN$ channel. There are several factors which contribute to the suppression of IC contributions at high Q^2 as compared to the SRC contributions. The main factors which should be emphasized are the energy dependence of the $A_{\Delta N \rightarrow NN}$ amplitude and the Q^2 -dependence of the electromagnetic $\gamma^* N \Delta$ transition form factors, as compared with the elastic $NN \rightarrow NN$ amplitude and the $\gamma^* N$ form factor respectively.

The $\Delta N \rightarrow NN$ amplitude is known to be dominated by the pion Reggeon exchange with the ρ -Reggeon which dominates at very high energies being a small correction up to the energies $\sqrt{s} \sim 30 \text{ GeV}$ [36]. Based on the rule that the energy dependence of the Feynman amplitude of the scattering process is defined by the spin, J of the exchanged particle as: $A \sim s^J$ one observes that the $\Delta N \rightarrow NN$ transition amplitude is suppressed at least by a factor $\propto 1/Q^2$ (at $Q^2 \geq 2 \text{ GeV}^2$) as compared to the elastic $NN \rightarrow NN$ amplitude leading to a similar suppression for IC contribution. In addition there is the experimental indication that the electromagnetic $\gamma^* N \Delta$ transition is decreasing faster with Q^2 as compared to the elastic $\gamma^* NN$ transition amplitude [37].

It follows from the above discussions that the smallest value of Q^2 required for effective studies of SRCs in the discussed class of experiments is $Q^2 \geq 1.5 \text{ GeV}^2$. The upper limit for Q^2 for studies of SRCs comes from the onset of color coherence phenomena at $Q^2 > 4 \text{ GeV}^2$, when FSIs will not maintain their energy independent characteristic for small angle hadronic rescattering (a discussion on color coherence is given in Sec.3).

Hence the optimal range for probing SRCs is

$$1.5 \leq Q^2 \leq 4 \text{ GeV}^2. \quad (5)$$

This range is large enough to check the validity of the Q^2 -independence of the extracted parameters of the SRCs. Jefferson Lab experiments at 6 GeV and very large missing momenta can reach the lower limit of this range and they would have only a very limited

access to the upper limit of Eqn. (5). With the upgrade of the beam energy the whole range of Eqn. (5) will be easily accessible for Jefferson Lab. This also permits a wider coverage of missing momenta and excitation energies of the recoil nuclear system.

2.4.2. Specific Reactions for Studies of Short Range Correlations The study of the (e, e') , $(e, e'N)$ and $(e, e'NN)$ reactions in the $(1.5 \leq Q^2 \leq 4 \text{ GeV}^2)$ range will allow a direct measurements of the nucleon momentum distributions and spectral functions out to large momenta, between 400 and 700 MeV/c. Here one expects that the nucleon degrees of freedom are dominant and one can explore short-range correlations. Although two nucleon correlations are expected to be the dominant part of the SRCs, triple and higher order SRCs (where more than two nucleons come close together) are significant as well - they are estimated to constitute $\sim 20\%$ of all SRCs [10]. At initial momenta $> 700 \text{ MeV/c}$ the non-nucleonic degrees of freedom should play an increasingly dominant role and for the first time one will be able to investigate them in detail.

The prime reactions for these investigations are:

- **Inclusive $A(e, e')X$ reaction at $x > 1$.** In the kinematic range of Eqn. (5), $A(e, e')X$ reactions at $x > 1$ proceed mainly by quasi-elastic scattering of electrons from bound nucleons. By increasing the values of x and Q^2 for these reactions, one can achieve a better discrimination between SRCs and long-range multi-step processes. This will allow the measurement of several average characteristics of SRCs: the probabilities of two-nucleon correlations in nuclei [8] and k_{\perp} -averaged longitudinal/light-cone momentum distributions in SRCs [38]. Extending measurements into the $x > 2$ region at sufficiently large values of Q^2 will allow us to probe the three-nucleon correlations. The signature of the dominance of 3N correlations in these reactions will be the onset of scaling of the cross section ratio of scattering from nuclei with $A > 3$ to that of $A = 3$ nucleus in the $x > 2$ region. Alternatively, one can look for multi-nucleon correlations by extending the Q^2 range of measurements for $x < 2$, and comparing heavy nuclei to deuterium. QCD evolution of the structure function leads to a shift of strength from high- x to lower- x values as Q^2 increases. If only two-nucleon correlations are present, then heavy nuclei will have no appreciable strength above $x = 2$ and the evolution should be essentially identical to the evolution of deuterium, and the ratio will remain constant. If, however, there is significant strength above $x = 2$ in heavy nuclei, coming from multi-nucleon correlations, then this strength will shift into the $x < 2$ region, and the ratio σ_A/σ_D will increase with Q^2 .

- **$d(e, e'pn)$.** While inclusive reactions have a large kinematic reach, they cannot probe the details of the structure of the SRCs. The starting point for these studies is the simplest exclusive reaction: $e + d \rightarrow e + p + n$. It will provide a test of the current understanding of the dynamics of electro-disintegration processes especially since the wave function of the deuteron is reasonably well known for a wide range of momenta ($\leq 400 \text{ MeV/c}$). Progress in building tensor polarized deuteron targets makes it feasible to study the polarization degrees of freedom of the disintegration reaction at sufficiently large Q^2 . In this case a direct separation of S and D waves is possible. Hence this

process will provide an ultimate test of our understanding of the short-distance NN interactions. In particular, it will allow us clearly discriminate between predictions based on approximations to the Bethe-Salpeter equation and light-cone approaches to the description of the deuteron as a two-nucleon relativistic system [39, 40]. Such studies, using the upgraded energies at Jefferson Lab will be a natural continuation of the present experimental program of electro-disintegration of the deuteron which is currently focused on studies in the momentum range of ≤ 400 MeV/c [41, 42, 43, 44].

- **$A(e, e'N)$ and $A(e, e'NN)$ with $A \geq 3$.** These reactions, with one nucleon produced along \vec{q} carrying almost the entire momentum of the virtual photon, allow measurements of the light-cone density matrix of the nucleus $\rho_A^N(\alpha, p_\perp)$ for large values of excitation energy, E_m , of the residual system. Within the SRC picture, it is expected that E_m increases with increasing initial momentum of the ejected nucleon. In the non-relativistic approximation, the average excitation energy is $\langle E_m \rangle \approx p_m^2/2m_N$, where \vec{p}_m is the missing momentum of the ejected nucleon. Measuring the E_m-p_m correlation at high Q^2 will be one of the signatures of scattering from SRCs.

Note that polarized ^3He targets used in $A(e, e'NN)N$ reactions will play a special role for probing SRCs due to the relative simplicity of the wave function and the unique possibility to probe the spin structure of pp and pn correlations. In particular, there exist kinematic regions where a minimum in the S-wave pp wave function can be explored, and the P-wave contribution can be isolated. These measurements will provide stringent tests of the structure of $A = 3$ systems and will test current interpretations of measurements of the ^3He form factors at large Q^2 .

- **$A(e, e'N_f N_b)$ reactions** with one nucleon (N_f) moving forward and the other (N_b) moving backward for nuclei with $A \leq 12$ can be used to investigate how the excitation energy is shared between nucleons. It is expected that the dominant contribution will originate from two-nucleon correlations. In this case N_b should carry most of the excitation energy. A comparison of the yields of (pp) , (pn) and (nn) processes will provide a detailed check of the mechanisms of the reaction and provide a quantitative comparison between the wave functions of two nucleon SRCs in the isospin zero and one channels (the former is expected to dominate by a factor ≥ 4 for a large range of momenta). In addition, if there is significant strength in multi-nucleon correlations, it should be manifest in the low excitation tail of the nuclear spectral function for large momenta of the ejected nucleon. This is best observed through the $(e, e'NN)$ reaction in which two nucleons are emitted in the backward direction relative to the virtual photon momentum [22]. In the high Q^2 regime, these reactions will allow us to study the parton structure of the three nucleon correlations at very high densities.

- **Quenching in the $A(e, e'N)$ scattering for $A \geq 10$.** The numerous $A(e, e'p)$ experiments at low $Q^2 \leq 0.3$ GeV² have observed the shell structure of nuclei for the momenta of residual nuclear system $\leq k_F$. At the same time they observed a significant (~ 0.5) suppression of the absolute cross sections as compared to shell model expectations. Jefferson Lab measurements on ^{12}C [45] and ^{16}O [46] targets at intermediate $Q^2 \sim 0.6 - 0.8$ GeV² suggest a quenching of about a factor of 0.7–

0.8. For large Q^2 ($\gtrsim 2 \text{ GeV}^2$) where virtual photons resolve individual nucleons the analysis [47, 48] of the current data including the Jefferson Lab data [49] indicate that this suppression has practically disappeared. Note however that the current comparison of quenching at different Q^2 should be considered as a semi-quantitative since different models of nucleon absorptions were used for treating $A(e, e'p)$ reactions at different Q^2 . Hence it is very important to perform similar measurements including a separation of the different structure functions at $Q^2 \sim 2 - 3 \text{ GeV}^2$ to investigate the Q^2 -dependence of the quenching. Such studies would be also of importance for the interpretation of the color transparency searches which will be discussed in Section 3.

Overall, a series of experiments at Jefferson Lab can provide a detailed knowledge of the nucleon component of the SRCs, mapping out both the strength and structure of two-nucleon (and multi-nucleon) SRCs for both light and heavy nuclei. With the proposed upgrade in beam energy, these studies will probe for the first time the quark substructure of the nucleon configurations at short space-time separations.

2.4.3. Experimental Requirements Carrying out the scientific program described above involves inclusive $A(e, e')$ and double coincidence $A(e, e'p)$ measurements as well as triple coincidence measurements of the $(e, e'pN)$ reactions on light nuclei, *e.g.* carbon. Inclusive measurements can be performed over a wide range at 6 GeV, and extended to the highest x -values with 11 GeV. The coincidence measurements are to be performed at the highest incident energy (11 GeV) and momentum transfer ($Q^2 = 4 - 6 \text{ GeV}/c^2$). These kinematical conditions are essential for covering the largest possible missing momentum range (up to 1 GeV/c). For this we need an electron spectrometer similar to that of the current high resolution spectrometer (HRS) of Hall A at Jefferson Lab, with extended momentum acceptance up to about 10 GeV/c, and a proton spectrometer with momentum acceptance up to about 2.5 GeV/c. For the triple coincidence measurements we also need a third large solid angle proton spectrometer and a neutron array. For protons, the BigBite spectrometer [50], which at its maximum current can detect particles in the momentum range of 250 – 900 MeV/c with moderate momentum resolution of $\Delta p/p = 0.8\%$, can be used. Behind the BigBite spectrometer a neutron counter array can be installed with a matching solid angle. This is basically the set-up proposed for an approved $(e, e'pN)$ experiment [51] with the current Jefferson Lab accelerator (at 5 GeV).

The limiting factor for luminosity in these measurements is the singles rate in the large solid angle detectors used to detect the recoil particles in coincidence with the knockout proton. Assuming that for the upgraded energies at 11 GeV the singles rate will be similar to that of the current one at 5 GeV beam, one can use 100 μA beam current and 1 mm carbon target to obtain the nuclear luminosity $\mathcal{L} = 6 \times 10^{36} \text{ cm}^{-2}\text{sec}^{-1}$. For the electro-disintegration of the deuteron we assume a target similar to the one used in the current Jefferson Lab experiments. The luminosity in this case (for 100 μA beam and 15 cm of 0.16 gr/cm² deuteron target) is: $\mathcal{L} = 3.7 \times 10^{37} \text{ cm}^{-2}\text{sec}^{-1}$.

For the differential cross section for the $d(e, e'p)n$ reaction, estimated in the missing

momentum range of 450 – 500 MeV/c in (almost) anti-parallel kinematics and at $Q^2 = 4\text{GeV}^2$, one obtains

$$\frac{d\sigma}{dE_e d\Omega_e d\Omega_p} = 1 \frac{pb}{\text{MeV sr}^2}. \quad (6)$$

Assuming $\Delta E_e = 50$ MeV and $\Delta\Omega_e = \Delta\Omega_p = 10$ msr, the counting rate is 650 events/hour. With a requirement of at least 500 events in 100 hours of beam time one will be able to measure the differential cross section as low as $0.005 \frac{pb}{\text{MeV sr}^2}$. Thus one will be able to measure well beyond 500 MeV/c region of missing momentum in the $d(e, e'p)n$ reaction.

To estimate the triple coincidence counting rate for the $A(e, e'pn)X$ reaction, we assume that events with high missing momenta ($p_m > 500$ MeV/c) originate mainly from two-nucleon SRCs. Under this condition, the measured differential cross section, in which the solid angle of the spectator neutron is integrated around the direction defined by the deuteron kinematics, can be approximated in the following way [51]:

$$\frac{d\sigma^A}{dE_e d\Omega_e \Omega_p} = K_0 \times a_2 \times Z \times \frac{d\sigma^d}{dE_e d\Omega_e \Omega_p} \quad (7)$$

where $\frac{d\sigma^d}{dE_e d\Omega_e d\Omega_p}$ is the differential cross section of the $d(e, e'p)n$ reaction [52], a_2 is defined through the ratio of cross sections for inclusive (e, e') scattering from heavy nuclei to deuterium, measured at $x > 1$ where the scattering from SRCs dominates, ($a_2(^{12}\text{C}) = 5.0 \pm 0.5$ [6]). K_0 is a kinematical factor related to the center of mass motion of np correlations in the nucleus and defined by the integration range of the spectator neutron solid angle. For K_0 we used a conservative estimate of 0.2 based on the neutron detector configuration designed for the experiment of Ref. [51]. Assuming additionally that the neutron detection efficiency is 50% one obtains a triple $(e, e'pn)$ coincidence rate of approximately 250 events/hour. With a requirement of at least 500 events in 100 hours of beam time a differential cross section as low as $0.02 \frac{pb}{\text{MeV sr}^2}$ can be measured.

The rate for the $A(e, e'pp)X$ reaction is more difficult to estimate since the pp correlations cannot be approximated by the high momentum part of the deuteron wave function. The ratio between the np and pp short range correlation contributions is poorly known and is one of the anticipated outcomes of the proposed measurements. For estimation purposes we assume that $2 \leq (np)/(pp) \leq 4$. This assumption is based mainly on counting the isospin degrees of freedom.

2.5. Quark Structure of Short-Range Correlations - Study of Superfast Quarks

The discovery of Bjorken scaling in the late 1960's [53] was one of the key steps in establishing QCD as the microscopic theory of strong interactions. These experiments unambiguously demonstrated that hadrons contain point-like constituents—quarks and gluons (see e.g. [54, 33]). In the language of quark-partons, the explanation of the observed approximate scaling was remarkably simple: a virtual photon knocks out a point-like quark, and the structure function of the target nucleon measured experimentally depends on the fraction x of the nucleon light cone momentum ($\equiv +$)

that the quark carries (up to $\log Q^2$ corrections calculable in pQCD). For a single free nucleon the Bjorken variable, $x = Q^2/2m_N\nu \leq 1$. It is crucial that the QCD factorization theorem be valid for this process, in which case the effects of all initial and final state interactions are canceled and the deep inelastic scattering can be described in terms of a light-cone wave function of the nucleon. Experimentally such scaling was observed, for a hydrogen target, for $Q^2 > 4 \text{ GeV}^2$ and $W > 2 \text{ GeV}$. Here $W^2 = -Q^2 + 2m_N\nu + m_N^2$ is the invariant mass squared of the hadronic system produced in the γ^*-N interaction.

Since the nucleus is a loosely bound system it is natural to redefine the Bjorken variable, for a nuclear target, as $x_A = AQ^2/2m_A\nu$ ($0 \leq x_A \leq A$), so that for scattering in kinematics allowed for a free nucleon at rest $x_A \approx x$. In the case of electron scattering from quarks in nuclei it is possible to have Bjorken- $x > 1$. This corresponds to the situation that a knocked-out quark carries a larger light-cone momentum fraction than a nucleon which is at rest in the nucleus. Such a situation could occur, for example, if the quark belongs to a fast nucleon in the nucleus. In the impulse approximation picture, the DIS structure function of a nucleus, $F_{2A}(x, Q^2)$, which directly relates to the nuclear quark distribution function, is expressed in terms of the nucleon structure function and the nuclear light-cone density matrix:

$$F_{2A}(x, Q^2) = \int_x^A \rho_A^N(\alpha_N, p_\perp) F_{2N}\left(\frac{x}{\alpha_N}, Q^2\right) \frac{d\alpha_N d^2p_\perp}{\alpha_N}, \quad (8)$$

where α_N is the light-cone momentum fraction of the nucleus carried by the interacting nucleon. Choosing $x \geq 1 + k_F/m_N \approx 1.2$ almost completely eliminates the contribution of scattering by quarks belonging to nucleons with momenta smaller than the Fermi momentum. Actually, the use of any realistic nuclear wave function would yield the result that the contribution of the component of the wave function with $k \geq k_F$ dominates at large Q^2 for values of x as small as unity. For these values of x , a quark must acquire its momentum from multiple nucleons with large relative momenta which are significantly closer to each other than the average inter-nucleon distance [10]. Thus, such superfast quarks in nuclei could arise from some kind of superdense configurations consisting either of a few nearby nucleons with large momenta or of more complicated multi-quark configurations. In particular, a comparison with Eqn. (8), which builds the nucleus from a distribution of essentially free nucleons, would provide a quantitative test whether the quarks in a bound nucleon have the same distribution function as in a free nucleon.

The kinematic requirement for detecting the signature of superfast quarks at $x > 1$ is to provide a value of Q^2 large enough that the tail of deep-inelastic scattering would overwhelm the contribution from quasi-elastic electron scattering from nucleons. One can estimate approximately the magnitude of the initial momentum of the nucleon, which is relevant in the DIS channel, expressing its projection in the \mathbf{q} direction through the produced invariant mass, W_N associated with scattering from a bound nucleon:

$$\frac{p_{initial}^z}{m} = 1 - x - x \left[\frac{W_N^2 - m^2}{Q^2} \right]. \quad (9)$$

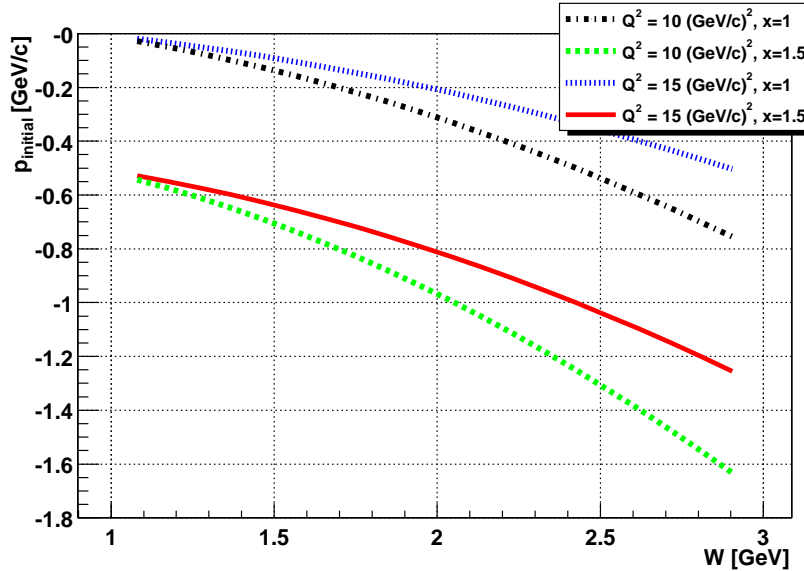


Figure 3. Relation between $p_{initial}^z$ and W_N^2 for $Q^2 = 10, 15$ (GeV/c) 2 and $x = 1, 1.5$

For a free nucleon, a given value of x and Q^2 automatically fixes the value of W_N^2 . In contrast, the internal motion of a bound nucleon allows a range of values of W_N^2 for given values of x, Q^2 . When average $W_N \geq 2$ GeV the deep inelastic contribution becomes dominant and the Bjorken scaling limit is reached. Figure 3 demonstrates that DIS can access extremely large values of initial momenta in nuclei at large Q^2 and x .

However, in order to probe these values of initial momenta the DIS contributions should dominate the quasi-elastic contribution. Figure 4 shows a calculation of the $A(e, e')X$ cross section at four different values of Q^2 . This figure illustrates that with increasing Q^2 the inelastic contribution remains dominant at increasingly larger values of x .

The first signal of the existence of superfast quarks will be the experimental observation of scaling in the region $x \geq 1$. Previous experimental attempts to observe such superfast quarks were inconclusive: the BCDMS collaboration [55] has observed a very small $x \geq 1$ tail ($F_{2A} \propto \exp(-16x)$), while the CCFR collaboration [56] observed a tail consistent with presence of very significant SRCs ($\sim \exp(-8x)$). A possible explanation for the inconsistencies is that the resolution in x at $x \geq 1$ of the high energy muon and neutrino experiments is relatively poor, causing great difficulties in measuring F_{2A} which is expected to vary rapidly with x . Therefore the energy resolution, intensity and energy of Jefferson Lab at 11 GeV may allow it to become the first laboratory to observe the onset of scaling and thereby confirm the existence of superfast quarks.

To estimate the onset of the Bjorken scaling we should extract the structure functions F_{2A} and F_{1A} from the cross section of the inclusive $A(e, e')X$ reaction. The cross section can be represented as follows:

$$\frac{d\sigma_A}{d\Omega_e dE'_e} = \frac{\sigma_{\text{Mott}}}{\nu} \left[F_{2A}(x, Q^2) + \frac{2\nu}{m_N} \tan^2(\theta/2) F_{1A}(x, Q^2) \right], \quad (10)$$

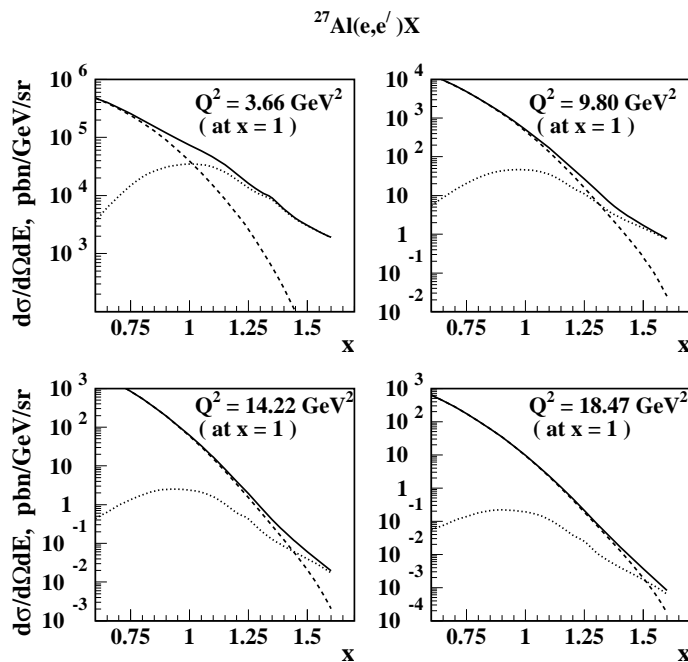


Figure 4. The differential $^{27}\text{Al}(e, e')X$ cross section as a function of x for fixed beam energy and scattering angle. The dotted line is the quasi-elastic contribution, the dashed line is the inelastic contribution, and the solid line is the sum of both contributions. Values of Q^2 are presented for $x = 1$.

where $F_{2A}(x, Q^2)$ and $F_{1A}(x, Q^2)$ are two invariant structure functions of nuclei. In the case of scaling, both structure functions become independent of Q^2 (up to $\log Q^2$ terms).

The experimental observable for scaling is the structure function, F_{2A} :

$$F_{2A}(x, Q^2) = \frac{d\sigma_A}{d\Omega_e dE'_e} \left(\frac{\nu}{\sigma_{\text{Mott}}} \right) \left[1 + \frac{1 - \epsilon}{\epsilon} \frac{1}{1 + R(x, Q^2)} \right]^{-1}, \quad (11)$$

where $\epsilon = [1 + 2(1 + \nu^2/Q^2) \tan^2(\theta/2)]^{-1}$ and $R \equiv \sigma_S/\sigma_T = (F_{2A}/F_{1A})(m_N/\nu)(1 + \frac{\nu^2}{Q^2}) - 1$. Figures 5 and 6 display calculations [58, 59] for deuteron and iron targets. Figure 5 demonstrates that at high Q^2 calculations become sensitive to the binding modification of the DIS structure function of the nucleons. To appreciate the size of the possible modification we used one of the models (color screening model of Ref. [60]) which describes reasonably well the nuclear EMC effect at $x < 1$ (see Sec. 2.6.1 for details). The calculations for ^{56}Fe show that the onset of scaling (Q^2 -independence) at $x = 1$ is expected at values of Q^2 as low as 5 – 6 GeV^2 . At $x = 1.5$ the onset of scaling depends strongly on the underlying model of SRCs and may occur already at $Q^2 \sim 10 \text{ GeV}^2$.

Figure 6 shows results obtained using three different models describing the ($A > 3$) nuclear state containing the superfast quark. In the first model, the momentum of the target nucleon in the nucleus is assumed to be generated by a mean field nuclear interaction only (dotted line). In the second, the high momentum component of the

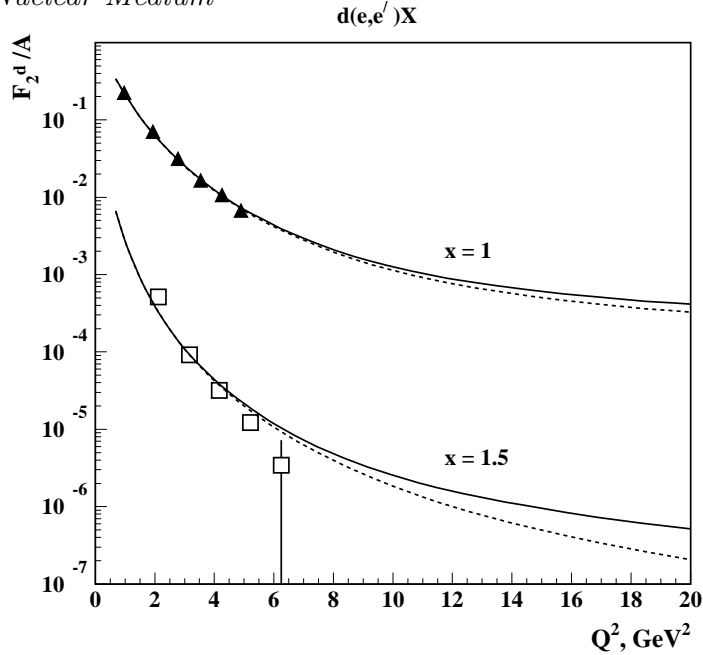


Figure 5. F_{2d}^d/A as a function of Q^2 for $x = 1$ and $x = 1.5$. Solid lines correspond to the light-cone calculation of Ref. [22] with no modification of the nucleon structure function. Dotted lines account for the binding modification of the nucleon DIS structure functions within the color screening model discussed in Sec. 2.6.1. No binding modification of elastic structure functions are considered. The data are from Ref. [57].

nuclear wave function is calculated using a two-nucleon short range correlation model (solid lines). Within this approximation the variations of the structure functions with x will be the same for deuteron and $A > 2$ targets at large values of Q^2 . In the third model, the multi-nucleon correlation model (dashed lines) of Ref. [61] is used. This model agrees reasonably well with recent measurements of the nuclear structure functions by the CCFR collaboration [56] but yields a significantly larger quark distribution than the one reported by the BCDMS collaboration [55].

Figure 7 represents the A -dependence of F_{2A} , which emphasizes that the use of large nuclei and large values of x would allow the significant study of the models of short-range correlations.

2.5.1. Experimental Requirements The physics program described above involves extending current inclusive scattering measurements at Jefferson Lab to the highest possible values of Q^2 at $x \geq 1$. The extension to higher Q^2 values requires the detection of high momentum electrons over a wide angular range $\theta \leq 60^\circ$. To reach the largest possible x values, we need to detect extremely high energy electrons at angles up to 30° . In both cases the measurements will require high luminosity, excellent pion rejection and a moderate ($\sim 10^{-3}$) momentum resolution. We use the measurement of the structure function $F_2(x, Q^2)$ for nuclei, as well as the ratio between Aluminum and Deuterium, as an example of a possible experiment that can be carried out with the Jefferson Lab upgrade. The extension to the highest possible Q^2 values, necessary to reach scaling and

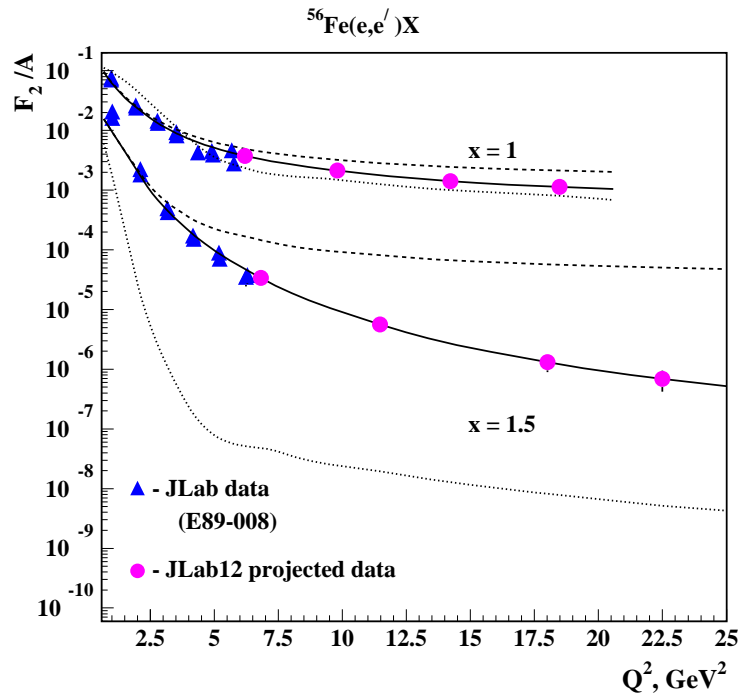


Figure 6. Prediction of the onset of scaling for $^{56}\text{Fe}(e, e')X$ scattering. The data are from Ref. [11] and the curves are the mean-field (dotted), two-nucleon SRCs (solid) and multi-nucleon SRCs (dashed) models, as described in the text.

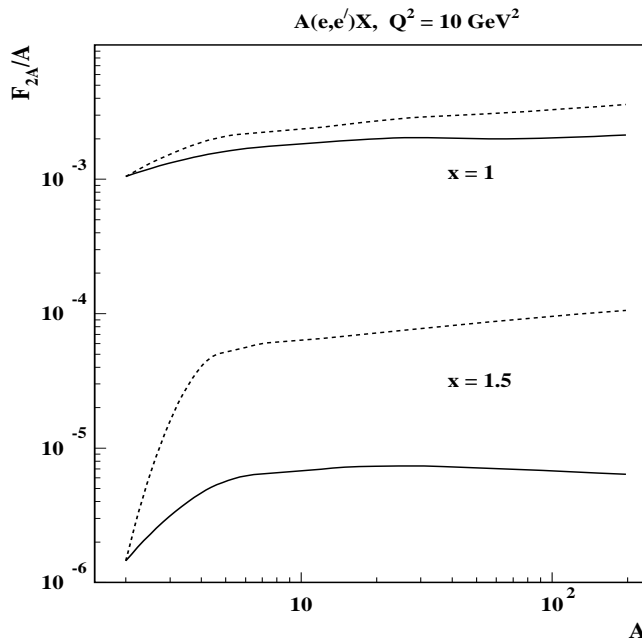


Figure 7. A-dependence of the structure function. The solid curve includes only two-nucleon SRCs, while the dashed curve includes multi-nucleon SRC contributions.

probe the quark distributions, can be performed using the equipment proposed for either Halls A or C at Jefferson Lab. The extension to the highest possible x values, where sensitivity to multi-nucleon correlations is greatest, requires the detection of electrons

with energies approaching the beam energy, and will require a very high momentum spectrometer, such as the proposed SHMS in Hall C.

In order to estimate the feasibility of these measurements at large values of x we have estimated count rates for Deuterium and Aluminum targets. The incident beam energy is assumed to be 11 GeV and a beam current of $60\mu A$ is used. We used a 10 cm long Deuterium target which corresponds to 1.5% of a radiation length. This implies a luminosity of $1.9 \cdot 10^{38} \text{s}^{-1} \text{cm}^{-2}$. These luminosities are currently used in many experiments at Jefferson Lab and do not pose any technical problems. For the Aluminum target we assumed a thickness of 0.5 cm which corresponds to a 6% radiator. This target will also have to be cooled but this should not pose any special problems. For the Aluminum target we then obtain a luminosity of $1.2 \cdot 10^{37} \text{s}^{-1} \text{cm}^{-2}$. We assume a solid angle of 10 msr and an expected momentum resolution of $\approx 10^{-3}$. These properties are certainly satisfied by the spectrometers proposed as part of the Jefferson Lab energy upgrade.

The pion rates have been estimated using the code EPC [62] and a parameterization of SLAC experimental data on pion yields. The problem in these estimates lies in the fact that the kinematics measured at SLAC have very little overlap with those examined here. Similarly the parameterizations employed in the code EPC are not optimized for this kinematical region. We therefore use the yields obtained only as a rough guide. In a real experiment proposal these models would need to be refined. Data from the approved $x > 1$ measurement at 6 GeV [12] will allow us to refine the pion and charge-symmetric background rate estimates.

The count rates have been evaluated for an bin size of $\Delta x = \pm 0.1$. The obtained rates for Deuterium are listed in Table 1 and the ones for Aluminum in Table 2. The cross sections come from the calculations shown in Figs. 5 and 6, (with multi-nucleon correlations included for the Aluminum). For these estimates, we have not included radiative effects.

θ_e	$Q^2(\text{GeV}/c)^2$	$\frac{d\sigma}{d\Omega d\nu} [\frac{nb}{sr \cdot \text{GeV}/c}]$	events/hour
5	1.06	1.24E+5	4.30E+7
10	3.87	4.48E+1	4.65E+4
20	11.47	3.74E-2	6.53E+1
30	18.01	2.07E-3	3.35
40	22.5	4.37E-4	5.58E-1

Table 1. Cross Sections and Count Rates for Deuterium, $x = 1.5$, including correlations.

The rate estimates indicate that for Deuterium the highest practical Q^2 value is about $Q^2 = 18 (\text{GeV}/c)^2$ while the count rate from Aluminum is still quite large at $Q^2 = 23 (\text{GeV}/c)^2$ with the experimental conditions described above. If we use the cross section with only two-body SRCs included, the rate will be significantly reduced,

θ_e	Q^2 (GeV/c) ²	$\frac{d\sigma}{d\Omega dv} [\frac{nb}{sr \cdot GeV/c}]$	events/hour
5	1.06	7.37E+6	1.60E+8
10	3.87	4.83E+3	3.13E+5
20	11.47	2.06E+1	2.25E+3
30	18.01	2.20	2.22E+2
40	22.5	6.57E-1	5.08E+1

Table 2. Cross Sections and Count Rates for Aluminum, $x = 1.5$, including correlations.

but we should still be able to approach $Q^2 = 23$ (GeV/c)². In all these cases we will reach Q^2 values where we are clearly dominated by the inelastic processes at $x > 1$.

2.6. Tagged Structure Functions

Understanding the role of the quark-gluon degrees of freedom in the hadronic interaction is tied strongly to understanding the dynamics responsible for modification of the quark-gluon structure of bound nucleons as compared to free nucleons. These dynamics at present are far from understood, however. Almost two decades after the discovery of the nuclear EMC effect [15] and increasingly precise measurements [63, 64, 65, 66, 67] of the ratios of structure functions of nuclei and the deuteron, we still know only that this effect requires the presence of *some* non-nucleonic degrees of freedom in nuclei. No consensus has been reached on the origin of these components.

The x -dependence of the effect, while non-trivial, is rather smooth and has the same basic shape for all nuclei, making it easy to reproduce using a wide range of models with very different underlying assumptions. The only additional constraint available to date comes from measurements of the A -dependence of the sea distribution in Drell-Yan reactions[21], which poses a problem for several types of models. The combination of the inclusive DIS and Drell-Yan experiments is still not sufficient to identify unambiguously the origin of the EMC effect. Inclusive experiments at Jefferson Lab, after the upgrade, will considerably improve our knowledge of the EMC effect by (i) measuring the EMC effect for the lightest nuclei [68], (ii) studying the isotopic dependence of the effect, and (iii) separating the different twists in the EMC effect. Though such experiments will be very important, they are unlikely to lead to an unambiguous interpretation of the EMC effect. New experiments involving more kinematical variables accessible to accurate measurements are necessary to overcome this rather unsatisfactory situation.

We propose that studying semi-inclusive processes involving a deuteron target,

$$e + d \rightarrow e + N + X, \quad (12)$$

in which a nucleon is detected in the target deuteron fragmentation region, may help to gain insight into the dynamics of the nuclear structure function modification [60, 69, 70, 71, 72]. Further important information could be obtained by studying the production of Δ -isobars and excited baryons in similar kinematics. Although we focus the discussion

here on the simplest case of a deuteron target, clearly similar experiments using heavier nuclei ($A = 3$, $A = 4$) would provide additional information.

A glimpse of the information that may be obtained from such experiments has already been provided by analyses of the experimental data on deep-inelastic neutrino scattering off nuclei [73, 74]. Even with poor statistics, these experiments have shown that structure functions, tagged by protons produced in the backward hemisphere, are different from those determined in inclusive scattering.

The semi-inclusive experiments which we contemplate should be able to answer the following questions: What is the smallest inter-nucleon distance (or largest relative momentum) for which the two nucleons in the deuteron keep their identities? What new physics occurs when this identity is lost? What is the signal that an explicit treatment of nuclear quark and gluon degrees of freedom is necessary? How much do the measured effective bound structure functions F_2 differ from those of free nucleons? Studying this difference will lead us to a better understanding of the dynamics behind nuclear binding effects and their relation to QCD.

The tool which allows us to control the relevant distances in the deuteron is the knowledge of the momentum of the tagged (backward) nucleon. The dependence of the semi-inclusive cross section on this variable will test the various assumptions regarding the lepton interaction with one nucleon while it is in a very close proximity to another nucleon. These very same assumptions are the ones that underlie the different models of the EMC effect. The study of the semi-inclusive reaction using a deuteron target will permit important insights into the deepest nature of many-baryon physics.

2.6.1. Theoretical Predictions for the EMC effect The **first group** of models, referred to as binding models, makes the simplest assumption regarding the lepton-nucleon interaction in a nucleus, namely, that nucleons maintain their nucleonic character. In these models, the nuclear EMC effect is caused by the effects of nuclear binding, and the inclusive structure function data can be understood in terms of conventional nuclear degrees of freedom—nucleons and pions—responsible for nuclear binding [69, 75, 76, 77, 78, 79, 80, 81, 82, 83, 84]. The nuclear cross section is then expressed as a convolution of the nuclear spectral function with the structure function of a *free* nucleon (Eqn. (8)). The off-mass-shell effect (if present at all) in these models constitutes a small part of the EMC effect, while the pion contribution is simply added to the contribution given by Eqn. (8).

The use of the standard, conventional meson-nucleon dynamics of nuclear physics is not able to explain both the nuclear deep-inelastic and the Drell-Yan data. One can come to this conclusion using the light-cone sum rules for the nuclear baryonic charge and the light-cone momentum [22]. Another approach [85, 86] is to use the Hugenholtz-van Hove theorem [87] which states that nuclear stability (vanishing of pressure) causes the energy of the single particle state at the Fermi surface to be $m_A/A \approx 0.99m_N$. In light front language, the vanishing pressure is achieved by setting $P^+ = P^- = m_A$. Since $P^+ = \int dk^+ f_N(k^+)k^+$ and the Fermi momentum is a relatively small value the

probability $f_N(k^+)$ for a nucleon to have a given value of k^+ must be narrowly peaked about $k^+ = 0.99m_N \approx m_N$. Thus, the effects of nuclear binding and Fermi motion play only a very limited role in the bound nucleon structure function. The resulting function must be very close to that of a free nucleon unless some quark-gluon effects are included. In this approach some non-standard explanation involving quark-gluon degrees of freedom is necessary.

Attempts to go beyond the simplest implementation of pion cloud effects have been made in Ref. [88], where recoil effects were taken into account. As a result it was argued that the predicted pion excess based on conventional correlated nuclear theory is not in conflict with data on the Drell Yan process or with the nuclear longitudinal response function. (Note that the pion enhancement enters in these two processes in a different way as the integrands of the integral over the pion light cone fraction, y_π , have different y_π dependence.) What does appear to be ruled out, however, are RPA theories in which there are strong collective pion modes [88]. At the same time the presence of pions on the level consistent with the Drell-Yan data does not allow us to reproduce the EMC effect (in a way consistent with the energy momentum sum rule) without introducing an ultrarelativistic mesonic component in the nucleus wave function. Each meson's light-cone fraction in the wave function is ≤ 0.03 but, taken together, the mesons carry $\sim 4\%$ of the light-cone fraction of the nucleus.

The **second group** of models represents efforts to model the EMC effect in terms of *off-mass-shell* structure functions, which can be defined by taking selective non-relativistic or on-shell limits of the virtual photon-off-shell nucleon scattering amplitude [89, 90, 91]. For example, the structure function of a bound nucleon of four-momentum p can depend on the variable $\gamma \cdot p - m$ [81]. Such terms should enter the calculation of the structure function only in the form of multi-nucleon contact interactions, so these models represent a parameterization of a variety of dynamical multi-nucleon effects. A microscopic, quark-level mechanism which can lead to such a modification is provided by the quark-meson coupling models [92, 93, 94], in which quarks confined in different nucleons interact via the exchange of scalar and vector mesons. Here the wave functions of bound nucleons are substantially different than those of free nucleons, even though the quarks are localized.

The **third group** of models assume that the main phenomenon responsible for the nuclear EMC effect is a modification of the bound state wave function of individual nucleons. In these models, the presence of extra constituents in nuclei or clustering of partons from different nucleons is neglected. Considerable modification of the bound nucleon structure functions at different ranges of x are predicted by these models. Two characteristic approaches are the color screening model of suppression of point-like configurations in bound nucleons [22, 60] and models of quark delocalization or dynamical rescaling [95, 96, 97, 98, 99]. These models do not include possible effects of partial restoration of chiral symmetry which would result in modification of the pion cloud at short internucleon distances.

The *color screening* models start from the observation that the point-like

configurations (PLCs) in bound nucleons are suppressed due to the effects of color transparency [22, 60, 100]. Based on the phenomenological success of the quark counting rules for $F_{2N}(x, Q^2)$ at large x it is further assumed that three quark PLCs give the dominant contribution at $x \geq 0.6$ and $Q^2 \geq 10 \text{ GeV}^2$. The suppression of this component in a bound nucleon was assumed to be a main source of the EMC effect in inclusive deep-inelastic scattering in Ref. [60]. The size of the effect was estimated to be proportional to the internal momentum of the target k (to the virtuality of the interacting nucleon) [60]:

$$\delta_A(\mathbf{k}^2) = (1 + z)^{-2}, \quad z = (\mathbf{k}^2/m_N + 2\epsilon_A)/\Delta E_A, \quad (13)$$

where $\Delta E_A = \langle E_i - E_N \rangle \approx m^* - m_N$, is the energy denominator characteristic of baryonic excitations. For $m^* = 1.5 - 1.7 \text{ GeV}$ the model reproduces reasonably the existing data on the EMC effect. Note that the considered suppression does not lead to a noticeable change in the average characteristics of nucleons in nuclei [60]: for example, PLC suppression of Eqn. (13) will lead to only 2% suppression of the cross section for high Q^2 scattering off a bound nucleon in quasi-free kinematics at $x = 1$ [59].

In *quark delocalization/rescaling* models it is assumed that gluon radiation occurs more efficiently in a nucleus than in a free nucleon (at the same Q^2) due to quark delocalization in two nearby nucleons. It is natural to expect that such a delocalization will grow with decreasing inter-nucleon distance. Within this model the effective structure function of the nucleon can be written as:

$$F_{2N}^{\text{eff}}(x, Q^2) = F_{2N} \left(x, Q^2 \xi(Q^2, k) \right), \quad (14)$$

where $\xi(Q^2)$ is estimated from the observed EMC effect in inclusive deep inelastic cross sections, and its Q^2 -dependence is taken from the generic form of the QCD evolution equations. The k -dependence in $\xi(Q^2, k)$ is modeled based on the assumption that the quark delocalization grows with increasing virtuality of a bound nucleon [72].

In the above classes of models the cross section for fast backward nucleon production in the reaction of Eqn. (12) can be represented as follows [72]:

$$\frac{d\sigma^{eD \rightarrow epX}}{d\phi dx dQ^2 d(\log \alpha) d^2 p_\perp} \approx \frac{2\alpha_{em}^2}{xQ^4} (1 - y) S(\alpha, p_\perp) F_{2N}^{\text{eff}}(\tilde{x}, \alpha, p_\perp, Q^2), \quad (15)$$

where $S(\alpha, p_\perp)$ is the nucleon spectral function of the deuteron, and F_{2N}^{eff} is the effective structure function of the bound nucleon, with $\tilde{x} \equiv x/(2 - \alpha)$. The variable $\alpha = (E_s - p_{sz})/m_N$ is the light-cone momentum fraction of the backward nucleon with p_{sz} negative for backward nucleons. Both spectral and structure functions can be determined from the particular models discussed above [72].

An alternative scenario to the models discussed above is based on the idea discussed since the 1970's that two (three) nucleons coming sufficiently close together may form a kneaded multiquark state [101, 102, 103, 104, 105, 106, 107, 108, 109, 110, 111]. An example of such a state is a bag of six quarks. Multiquark cluster models of the EMC effect were developed in a number of papers [105, 114, 113, 114]). In **six-quark** ($6q$) models electromagnetic scattering from a $6q$ configuration is determined from a

convolution of the structure function of the $6q$ system with the fragmentation functions of the five- (or more, in general) quark residuum[70]. These types of models cannot be represented through the convolution of a nucleon structure function and spectral function as in Eqn. (15). Since the quarks in the residuum depend on the flavor of the struck quark, one finds[71]:

$$\frac{d\sigma^{eD \rightarrow epX}}{d\phi dx dQ^2 d(\log \alpha) d^2 p_\perp} \approx \frac{2\alpha_{em}^2}{Q^4} (1-y) \sum_i x e_i^2 V_i^{(6)}(x) \frac{\alpha}{2-x} D_{N/5q}(z, p_\perp), \quad (16)$$

where the sum is over quark flavors. Here $V_i^{(6)}$ is the distribution function for a valence quark in a $6q$ cluster, and $D_{N/5q}(z, p_\perp)$ is the fragmentation function for the $5q$ residuum, i.e., the probability per unit z and p_\perp for finding a nucleon coming from the $5q$ cluster. The argument z is the fraction of the residuum's light-cone longitudinal momentum that goes into the nucleon: $z = \frac{\alpha}{2-x}$.

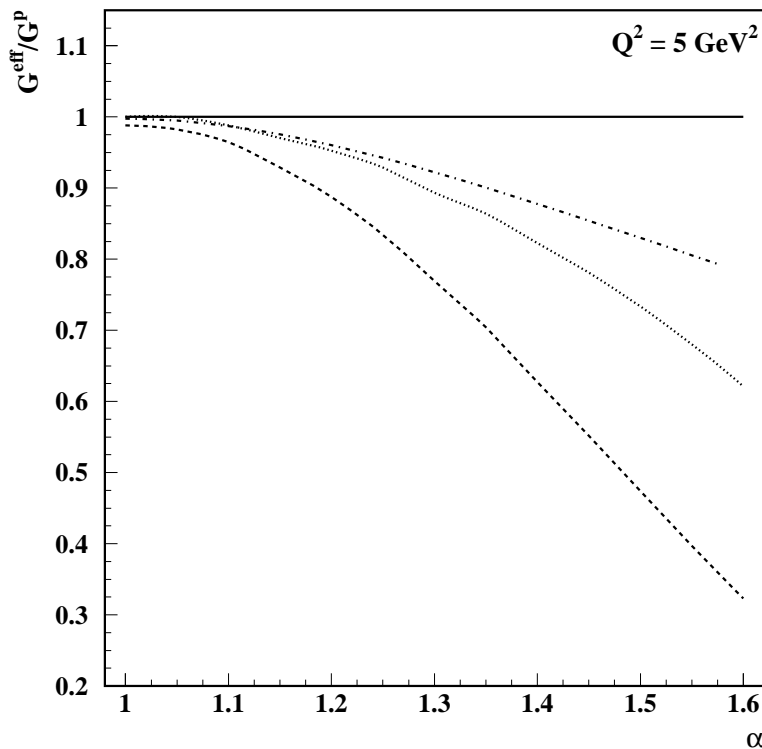


Figure 8. The α -dependence of $G(\alpha, p_\perp, x_1, x_2, Q^2)$, with $x_1 = x/(2-\alpha) = 0.6$ and $x_2 = x/(2-\alpha) = 0.2$. $G^{eff}(\alpha, p_\perp, x_1, x_2, Q^2)$ is normalized to $G^{eff}(\alpha, p_\perp, x_1, x_2, Q^2)$ calculated with the free nucleon structure function with $p_\perp = 0$. The dashed line is the color screening model [60], dotted is the color delocalization model [95], and dot-dashed the off-shell model [89].

2.6.2. Observables Guided by the expectation [72] that final state interactions should not strongly depend on x , Eqn.(15) suggests it is advantageous to consider the ratio of cross sections in two different bins of \tilde{x} : one where the EMC effect is small ($\tilde{x} \sim 0.1-0.3$) and one where the EMC effect is large ($\tilde{x} \sim 0.5-0.6$) [22, 60]. We suggest therefore

measuring the ratio G , defined as:

$$\begin{aligned} G(\alpha, p_{\perp}, x_1, x_2, Q^2) &\equiv \frac{d\sigma(x_1, \alpha, p_{\perp}, Q^2)}{dx dQ^2 d(\log \alpha) d^2 p_{\perp}} \bigg/ \frac{d\sigma(x_2, \alpha, p_{\perp}, Q^2)}{dx dQ^2 d(\log \alpha) d^2 p_{\perp}} \\ &= \frac{F_{2N}^{eff}(x_1/(2-\alpha), \alpha, p_{\perp}, Q^2)}{F_{2N}^{eff}(x_2/(2-\alpha), \alpha, p_{\perp}, Q^2)}. \end{aligned} \quad (17)$$

Since the function G is defined by the ratio of cross sections at the same α and p_{\perp} , any uncertainties in the spectral function cancel. This allows one to extend this ratio to larger values of α , thereby increasing the utility of semi-inclusive reactions. Figure 8 shows the α -dependence of $G(\alpha, p_{\perp}, x_1, x_2, Q^2)$ at $p_{\perp} = 0$ for several different models. The values of x_1 and x_2 are selected to fulfill the condition $x_1/(2-\alpha) = 0.6$ (large EMC effect in inclusive measurements) and $x_2/(2-\alpha) = 0.2$ (essentially no EMC effect). Note that while they yield similar inclusive DIS cross sections, the models predict significantly different values of the ratio function G .

From Eqn. (15) one further observes that in all models that do not require the mixing of quarks from different nucleons, the x -dependence of the cross section is confined (up to the kinematic factor $1/x$) to the argument of the tagged nucleon structure function, F_{2N}^{eff} . On the other hand, for $6q$ models the x -dependence reflects the momentum distribution in the six-quark configuration, Eqn. (16). As a result it is useful to consider the x -dependence of the observable defined as:

$$R = \frac{d\sigma}{dx dQ^2 d \log(\alpha) d^2 p_{\perp}} \bigg/ \frac{4\pi\alpha_{em}^2(1-y)}{xQ^4}. \quad (18)$$

For the convolution-type models discussed above, the ratio R is just the product of the spectral function, $S(\alpha, p_{\perp})$, and the effective nucleon structure function, $F_{2N}^{eff}(\tilde{x}, \alpha, p_{\perp}, Q^2)$. In the on-shell limit the x -dependence of R is therefore identical to that of the free nucleon structure function.

Figure 9 presents the x dependence of R normalized by the same ratio calculated using Eqn.(15) with F_{2N}^{free} . The calculations are performed for different models at $\alpha = 1.4$ and $p_{\perp} = 0$. Within the off-shell/covariant spectator model [89] R exhibits a relatively weak dependence on x , while $6q$ models predict a rather distinct x -dependence. Note that the models from the first group (binding models) does not produce any effect for this ratio. This ratio exposes a large divergence of predictions, all of which are obtained from models which yield similar EMC effects for inclusive reactions. Jefferson Lab at 11 GeV should therefore have a unique potential to discriminate between different theoretical approaches to the EMC effect, and perhaps reveal the possible onset of the $6q$ component of the deuteron wave function.

An important advantage of the reactions considered with tagged nucleons, in contrast to inclusive reactions, is that any experimental result will be cross checked by the dependence of the cross section on α and p_{\perp} . Figure 10 shows the accessibility of the scaling region as a function of incoming electron energy [71]. Values of x between the curves labeled by x_{\min} and x_{\max} can be reached in the scaling region for a given incoming electron energy E_e .

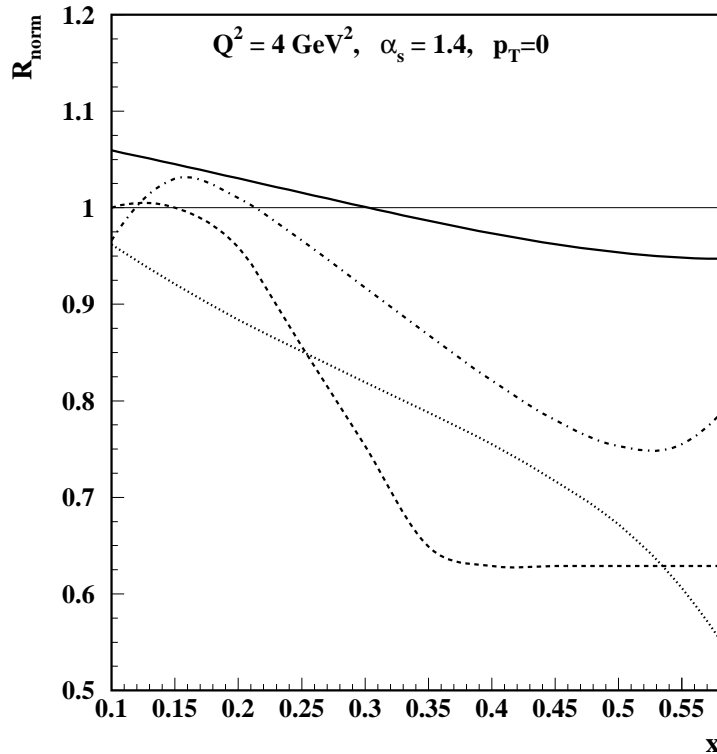


Figure 9. The x -dependence of the normalized ratio R defined in Eqn. (18). The solid, dashed, dotted and dot-dashed curves represent the predictions of off-shell (covariant spectator) [89], color screening [60], quark delocalization [95] and six-quark [71] models, respectively. The binding models (group one) predict the ratio of one - thin solid line.

2.6.3. Extraction of the “Free” Neutron DIS Structure Function Aside from providing a qualitatively new insight into the origin of the nuclear EMC effect per se, the measurements of the tagged events may also be useful for extracting the free neutron structure function from deuteron data. By selecting only the slowest recoil protons in the target fragmentation region, one should be able to isolate the situation whereby the virtual photon scatters from a nearly on-shell neutron in the deuteron. In this way one may hope to extract F_{2n} with a minimum of uncertainties arising from modeling nuclear effects in the deuteron.

One approach to extract the free F_{2n} is to extrapolate the measured tagged neutron structure function to the region of negative values of kinetic energy of the spectator proton||, where the pole of the off-shell neutron propagator in the PWIA amplitude is located ($E_{kin}^{pole} = -\frac{|\epsilon_D| - (m_n - m_p)}{2}$). The advantage of such an approach is that the scattering amplitudes containing final state interactions do not have singularities corresponding to on-shell neutron states. Thus, isolating the singularities through the extrapolation of effective structure functions into the negative spectator kinetic energy range will suppress the FSI effects in the extraction of the free F_{2n} [116]. Figure 11

|| This method is analogous to the Chew–Low procedure for extraction of the cross section of scattering off a pion[115].

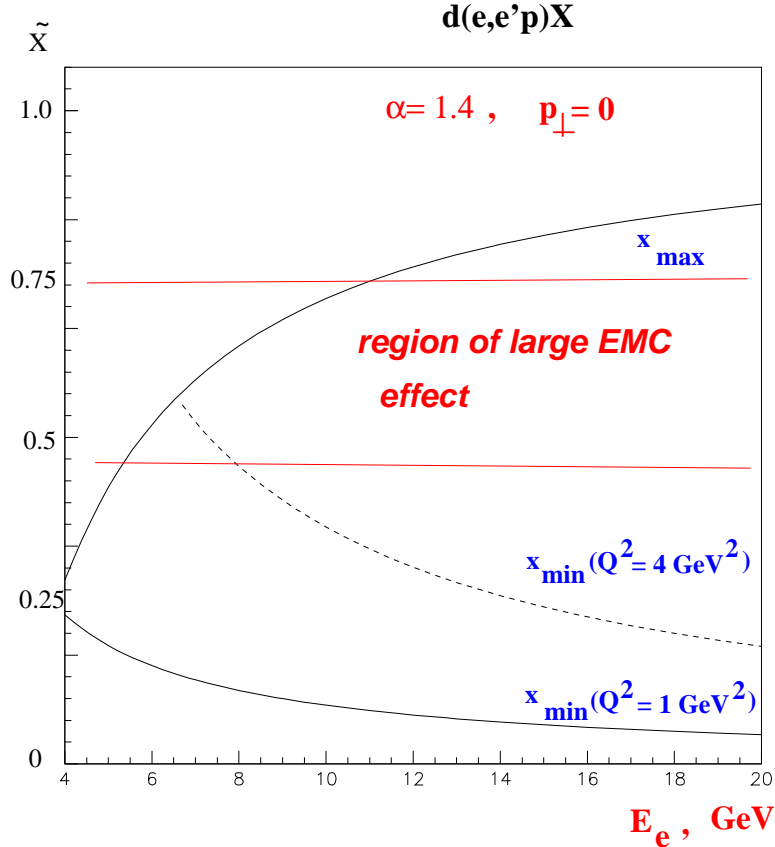


Figure 10. The scaling window for $\alpha = 1.4$. The upper curve is defined by the requirement that the mass of the produced final hadronic state $W \geq 2$ GeV.

demonstrates that such an extrapolation can indeed be done with the introduction of negligible systematic errors.

2.6.4. Experimental Objectives As described in the previous section, our goal is to measure the reaction $d(e, e'p_{\text{backward}})X$ over a large range in the electron variables (x , Q^2) and the backward proton kinematics (α , p_{\perp}). The proposed experiment would use the upgraded “CLAS++” (CEBAF Large Acceptance Spectrometer) with an 11 GeV beam to detect scattered electrons in coincidence with protons moving backward relative to the momentum transfer vector, \mathbf{q} . A large acceptance spectrometer is required since the proton is selected in spectator kinematics (small to moderate momentum up to 700 MeV/c anywhere in the backward hemisphere) and is uncorrelated with the electron direction. Scattered electrons will be detected by the upgraded forward spectrometer with two sets of Cerenkov counters, time of flight counters, three tracking regions and pre-shower and total absorption electromagnetic calorimeters for highly efficient electron/pion separation. Depending on the momentum range of interest, two different detector/target arrangements will be used for the detection of the backward-moving proton.

The first case involves the use of a dedicated integrated target-detector system with a 5 atmosphere deuterium gas cell as target (30 cm long and 0.5 cm diameter) and a

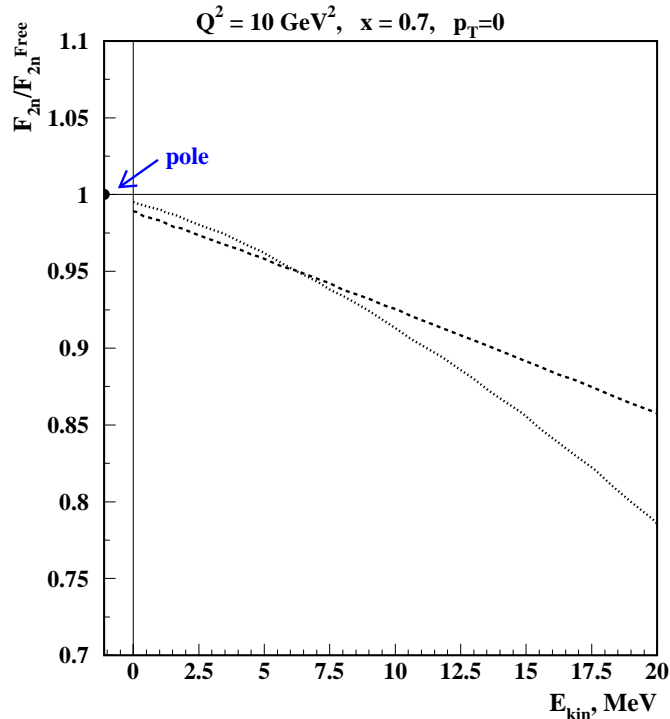


Figure 11. The E_{kin} dependence of the neutron structure function extracted from $d(e, e'p_{\text{backward}})X$ reactions within PWIA. The effective structure function is normalized by the on-shell neutron structure function. Dashed and dotted curves correspond to the calculation within Color Screening [60] and Color Delocalization [95] models, respectively.

multilayer GEM (Gas Electron Multiplier) detector surrounding the target cell. By minimizing all materials in the path of large angle tracks, the threshold for detection of backward-moving protons can be lowered to about 70 – 80 MeV/c. One expects that nucleon structure modifications and off-shell effects will be small at these momenta, and this method can be used to extract unambiguously the free neutron structure function $F_{2n}(x)$ up to very high values of x (≈ 0.8). This measurement is of fundamental importance, since presently our knowledge of the neutron structure function at high x is rather poor. At the same time, it will supply the “low momentum“ part of the nucleon momentum dependence of the effective off-shell structure function, F_{2n}^{eff} , and thus serve as a baseline for the non-nucleonic effects which are expected at higher proton momenta. This target-detector system is presently under development and will be used for an exploratory measurement at 6 GeV beam energy. Together with CLAS⁺⁺ and an 11 GeV beam at a luminosity of $0.5 \cdot 10^{34} \text{ cm}^{-2}\text{s}^{-1}$, a statistical precision of better than $\pm 5\%$ on F_{2n} out to the highest values of x would be obtained with 40 days of data taking.

In the second case, a central detector of CLAS⁺⁺, with superconducting solenoid, tracking and time-of-flight detectors would be used to measure backwards-going protons with momenta above 250 MeV/c. With these higher momenta, one achieves great sensitivity to modifications of the neutron structure because of the proximity of the

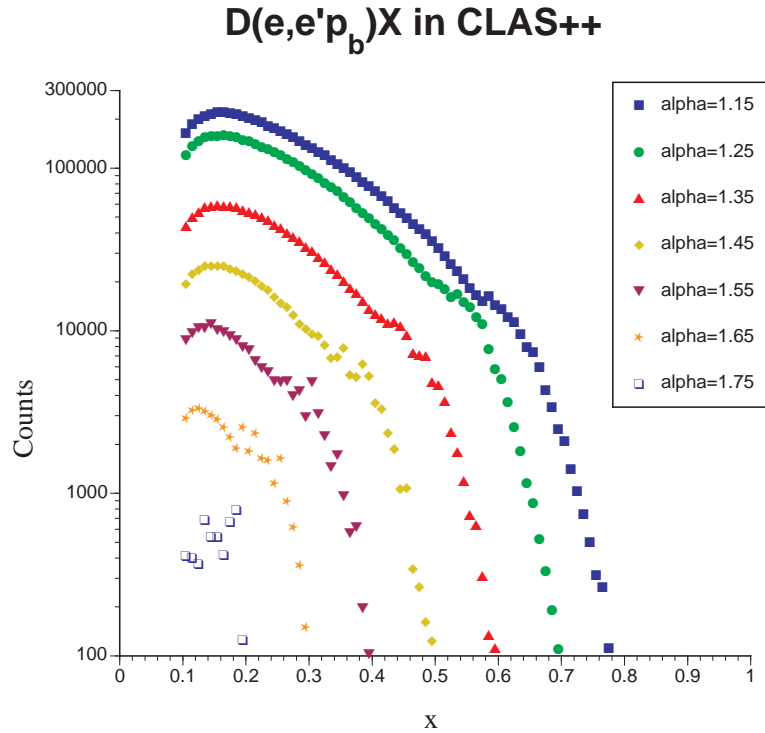


Figure 12. Kinematic coverage in Bjorken- x and proton light-cone fraction α_S for the high-momentum part of the proposed experiment. The count rates have been estimated for a 20 day run with the standard CLAS++ configuration.

“spectator” proton.

The dependence of the structure function $F_{2n}^{eff}(x/(2-\alpha), \alpha, p_{\perp}, Q^2)$ on the proton momentum from about 250 MeV/c to over 600 MeV/c can be extracted at fixed x and Q^2 . The experiment will simultaneously cover a large range in x and Q^2 , allowing detailed comparisons with the different models described in the previous section. Due to the higher momentum threshold, one can use a standard liquid deuterium target and the full CLAS++ luminosity of $10^{35} \text{ cm}^{-2}\text{s}^{-1}$.

Fig. 12 shows estimates of the expected number of counts for a 20 day run as a function of x for seven bins in the light-cone fraction α of the backward proton. One can clearly see the kinematic shift due to the motion of the struck neutron, which we can fully correct using the proton kinematics. It is clear that good statistics for a large range in x and in α (the highest bin corresponds to more than 600 MeV/c momentum opposite to the direction of the \mathbf{q} vector) would be obtained. Together with the low-momentum results, these data can be used to put the various models described in the previous section to a stringent test.

3. Observation of Color Coherent Phenomena at Intermediate Energies

3.1. Basic aspects of color coherence and color transparency

QCD displays some of its special characteristics as a theory involving $SU(3)$ -color by its prediction of novel effects in coherent processes. The basic idea is that the effects of gluons emitted by a color-singlet which is small-sized (or in a point-like configuration) are canceled if the process is coherent. This is because, if the process is coherent, one computes the scattering amplitude by summing the terms caused by gluon emissions from different quarks. The implication is that for certain hard exclusive processes, the effects of initial and/or final state interactions will be absent.

To observe color coherence effects it is necessary to find processes which are dominated by the scattering of hadrons in a PLC and hence have amplitudes that can be calculated using pQCD. A number of such processes have been suggested in the literature, and the corresponding QCD factorization theorems have been proven for them. These processes include diffractive pion dissociation into two high transverse momentum jets [117] and exclusive production of vector mesons [118, 119].

Experiments at HERA which studied exclusive production of vector mesons in deep inelastic scattering (recently reviewed in [120]), have convincingly confirmed the basic pQCD predictions – a fast increase of the cross section with energy at large Q^2 , dominance of the longitudinal photon cross section and a weaker t -dependence of the ρ -meson production at large Q^2 relative to J/ψ photoproduction.

A distinctive feature of processes such as di-jet and vector meson production is that, in the case of nuclear targets, the incoming $q\bar{q}$ pair does not experience attenuation for the range of x for which gluon shadowing is small ($x \geq 0.02$). This is the Color Transparency (CT) phenomenon. As a result, the amplitude of the corresponding nuclear coherent processes at $t = 0$, and the cross section of quasi-elastic processes are each proportional to the nucleon number A , a result which is vastly different from the results usually obtained in processes involving soft hadrons.

Color transparency, as predicted by pQCD, was directly observed in the Fermi Lab experiment E791 which investigated the exclusive coherent production of two jets in the process $\pi + A \rightarrow 2 \text{ jets} + A$ at $E_\pi = 500$ GeV. The observed A -dependence of the process [121, 122] is consistent with the predictions of [117], which lead to a seven times larger platinum/carbon ratio than soft physics would. The study of this reaction also allowed measuring the pion $q\bar{q}$ wave function [121, 122], which turned out to be close to the asymptotic one at $k_\perp \geq 1.5$ GeV/c. Evidence for color transparency effects was reported also in incoherent vector meson production in DIS scattering of muons [123].

Hence we conclude that the general concepts of CT in pQCD domain are now firmly established for high energy processes: the presence of PLCs in vector mesons and pions and the form of the small size $q\bar{q}$ dipole-nucleon interaction at high energies are well established experimentally¶

¶ At sufficiently small $x (\leq 0.01)$ which can be achieved at RHIC, HERA, and LHC, the quantum field

It is natural to apply the CT ideas to address the question of interplay of small and large distances in various high-momentum transfer processes at intermediate energies. This involves three key elements: (i) the presence of configurations of small transverse size in hadrons, (ii) the small size configurations not expanding as they exit the nucleus (i.e. a large coherence length) at high energies, which leads to the possibility of considering the small-sized configurations as frozen during the collision, and (iii) the weakness of the interaction of small color singlet objects at high energies (for example, for a small color $q\bar{q}$ dipole of transverse size r_t , the effective cross section is $\sigma_{\text{eff}} \sim r_t^2$). It also is vital that the experiment be performed with sufficient precision to be certain that no additional pions be created. This is necessary to maintain the exclusive or nearly exclusive nature of the experiment, which is required for the necessary quantum interference effects to dominate the physics. The considered effect in general is analogous to the reduction of the electromagnetic interaction strength of the electrically neutral Q^+Q^- dipole at small separations. However the uniqueness of QCD is in the prediction of the similar phenomena for color-neutral qqq configurations. Establishing the existence of color coherence effects for three-quark systems would verify the color SU(3) nature of QCD, and remains an important unmet challenge.

3.2. Goals For Intermediate Energy Studies

The major directions for study of CT related phenomena at Jefferson Lab are determined by the fact that one probes the transition from soft to hard QCD regime. These studies include:

- Determining the interplay between the contribution of large and small distances for specific processes.
- Studying the interaction cross section of small objects in kinematic regions for which quark exchanges may play the dominant role as compared to gluon exchanges (at high energies the two-gluon exchange in t -channel dominates).
- Studying the dynamics of wave packet expansion.

All of these aspects can be addressed if one considers the fundamental physics involved with the nucleon form factor at large Q^2 and the scattering amplitude for large angle hadron-nucleon elastic scattering. In QCD it is expected that at very large Q^2 the form factor and scattering amplitude are each dominated by contributions arising from the minimal Fock space components in the nucleon (hadron) wave function. Such components, involving the smallest possible number of constituents, are believed to be of a very small size, or to contain a PLC. To determine the values of Q^2 for which PLCs start to dominate, Brodsky [124] and Mueller [125] suggested the study of quasi-elastic hard reactions $l(h) + A \rightarrow l(h) + p + (A - 1)^*$. If the energies and momentum transfers are large enough, one expects that the projectile and ejected nucleon travel through the theory treatment of the CT predicts a gradual disappearance of the CT and the onset of the color opacity phenomenon.

nucleus as point-like (small size) configurations, resulting in a cross section proportional to A .

3.3. Challenges for intermediate energy studies

To interpret the physics of quasi-elastic reactions one has to address two questions:

- Can the PLCs be treated as a frozen during the time that the projectile is passing through the nucleus?
- At what momentum transfer do the effects of PLCs dominate in the elementary amplitude?
- Do they have small interaction cross sections?

These questions must be addressed if color transparency is to be studied at Jefferson Lab. If the momentum transfer is not large enough for the PLC to dominate or if the PLC is not frozen and expands, then there will be strong final state interactions as the PLC moves through the nucleus.

To appreciate the problems we shall discuss the effects of expansion in a bit more detail. Current color transparency experiments are performed in kinematic regions where the expansion of the produced small system is very important. In other words the length (the coherence length l_c) over which the PLC can move without the effects of time evolution changing the character of the wave function is too small, and this strongly suppresses any effects of color transparency [126, 127, 128, 129, 130, 131, 132]. The *maximal* value of l_c for a given hadron h can be estimated using the uncertainty principle: $l_c \sim \frac{1}{\Delta M} \frac{p_h}{m_h}$, in which ΔM is a characteristic excitation energy (for a small value of m_h one can write $l_c \approx \frac{2p_h}{\Delta M^2}$ with $\Delta M^2 = (m_{ex}^2 - m_h^2)$ where m_{ex}^2 is the invariant mass squared of the closest excited state with the additive quantum numbers of h (cf Eqn. (20)). Numerical estimates [126, 128, 129, 130, 131] show that, for the case of a nucleon ejectile, coherence is completely lost at distances $l > l_c \sim 0.3 - 0.5 \text{ fm} \times p_h$, where p_h is measured in GeV/c.

Two complementary languages have been used to describe the effect of the loss of coherence. Ref. [126] used the quark-gluon representation of the PLC wave function, to argue that the main effect is quantum diffusion of the wave packet so that

$$\sigma^{PLC,Q^2}(Z, Q^2) = (\sigma_{hard} + \frac{Z}{l_c}[\sigma - \sigma_{hard}])\theta(l_c - Z) + \sigma\theta(Z - l_c), \quad (19)$$

where $\sigma^{PLC}(Z, Q^2)$ is the effective total cross section for the PLC to interact at a distance Z from the hard interaction point. This equation is justified for the “hard stage” of time development in the leading logarithmic approximation when perturbative QCD can be applied [126, 133, 22, 134]. One can expect that Eqn. (19) smoothly interpolates between the hard and soft regimes, at least for relatively large transverse sizes of the expanding system ($\geq 1/2$ of the average size) which give the largest contribution to absorption.

The time development of the PLCs can also be obtained by modeling the ejectile-nucleus interaction using a baryonic basis for the PLC[135]:

$$\begin{aligned} |\Psi_{PLC}(t)\rangle &= \sum_{i=1}^{\infty} a_i \exp(iE_i t) |\Psi_i\rangle \\ &= \exp(iE_1 t) \sum_{i=1}^{\infty} a_i \exp\left(\frac{i(m_i^2 - m_1^2)t}{2p}\right) |\Psi_i\rangle, \end{aligned} \quad (20)$$

where $|\Psi_i\rangle$ are the eigenstates of the Hamiltonian with masses m_i , and p is the momentum of the PLC which satisfies $E_i \gg m_i$. As soon as the relative phases of the different hadronic components become large (of the order of one) the coherence is likely to be lost. It is interesting that numerically Eqns. (19) and (20) lead to similar results if a sufficient number of states is included in Eqn. (20) [135]. It is worth emphasizing that, though both approaches model certain aspects of the dynamics of the expansion, a complete treatment of this phenomenon in QCD is absent.

We next discuss the issue of the necessary momentum transfers required for PLCs to be prominent. For electromagnetic reactions this question is related to the dominance of PLCs in the electromagnetic form factors of interacting hadrons. The later can be studied by considering the applicability of perturbative QCD in calculating the electromagnetic form factors. Current analyses indicate that the leading twist approximation for the pion form factor could become applicable (optimistically) at $Q^2 \geq 10 - 20 \text{ GeV}^2$; see e.g. Ref. [136, 137]. For the nucleon case larger values of Q^2 may be necessary. However this does not preclude PLCs from being relevant for smaller values of Q^2 . In fact, in a wide range of models of the nucleon, such as constituent quark models with a singular (gluon exchange type) short-range interaction or pion cloud models, configurations of sizes substantially smaller than the average one dominate in the form factor at $Q^2 \geq 3 - 4 \text{ GeV}^2$; see Ref. [138]. The message from QCD sum rule model calculations of the nucleon form factor is more ambiguous.

For hadron-nuclear reactions the question of the dominance of PLCs is related to theoretical expectations that large angle hadron-hadron scattering is dominated by the hard scattering of PLCs from each hadron. However this question is complex because one is concerned with placing larger numbers of quarks into a small volume. Irregularities in the energy dependence of pp scattering for $\theta_{c.m.} = 90^\circ$, and large spin effects, have led to suggestions of the presence of two interfering mechanisms in this process [139, 140], corresponding to interactions of the nucleon in configurations of small and large sizes. See the review [141].

The difficulties involved with using hadron beams in quasi-elastic reactions can be better appreciated by considering a bit of history. The very first attempt to observe color transparency effects was made at the AGS at BNL [142]. The idea was to see if nuclei become transparent with an increase of momentum transfer in the $p+A \rightarrow p+p+(A-1)$ reaction. As a measure of transparency, T , they measured the ratio:

$$T = \frac{\sigma^{\text{Exp}}}{\sigma^{\text{PWIA}}}, \quad (21)$$

where σ^{Exp} is the measured cross section and σ^{PWIA} is the calculated cross section using plane wave impulse approximation (PWIA) when no final state interaction is taken

into account. Color transparency is indicated if T grows and approaches unity with increasing energy transfer.

The experiment seems to support an increase of transparency at incident proton momentum $p_{inc} = 6 - 10$ GeV/c as compared to that at $E_p = 1$ GeV; see the discussion in [143]. The magnitude of the effect can be easily described in color transparency models which include the expansion effect. The surprising result of the experiment was that with further increase of momentum, (≥ 11 GeV/c), T decreases. The first data from a new $(p, 2p)$ experiment, EVA[144], at $p_{inc} = 6 - 7.5$ GeV/c confirmed the findings of the first experiment [142] and more recently EVA has reported measurements in a wider momentum range up to 14 GeV/c. The data appear to confirm both the increase of transparency between 6 and 9 GeV/c and a drop of transparency at 12 and 14 GeV/c [145].

The drop in the transparency can be understood as a peculiarity of the elementary high momentum transfer pp scattering amplitude, which contains an interplay of contributions of PLCs and large size configurations as suggested in [139, 140]. A description of the drop in transparency based on these ideas was presented in Ref. [146]. However, it is evident that the interpretation of any experiment would be simplified by using an electron beam.

The most general way to deal with each of the challenges mentioned here is to perform relevant experiments using electrons at the highest possible values of energy and momentum transfer.

3.4. Color Transparency in $(e, e'N)$ and $(e, e'NN)$ Reactions

The first step is to measure a transparency similar to that of Eqn. (21) using electroproduction reactions. The first electron $A(e, e'p)$ experiment looking for color transparency was NE-18 performed at SLAC [147, 148]. The maximum Q^2 in this experiment is ≈ 7 GeV², which corresponds to $l_c \leq 2$ fm. For these kinematics, color transparency models which included expansion effects predicted a rather small increase of the transparency; see for example [22]. This prediction is consistent with the NE-18 data. However these data are not sufficiently accurate either to confirm or to rule out color transparency on the level predicted by realistic color transparency models. Recent Jefferson Lab experiments [49, 149] have been performed up to $Q^2 = 8$ GeV², and no effects of color transparency have been observed (see Fig. 13). However, models of color transparency which predict noticeable effects in the (p, pp) reaction include versions which can also lead to almost no effects in electron scattering. In those models, the effects of expansion are strong for the lower energy final state wave functions, but do allow some color transparency to occur for the initial state wave function. At $Q^2 = 8$ GeV², the momentum of the proton ejected in electron scattering is about 5 GeV/c, which is still lower than the lowest momentum, 6 GeV/c used at BNL. One needs to achieve a Q^2 of about 12 GeV² to reach a nucleon momentum for which BNL experiment observed an increase of the transparency.

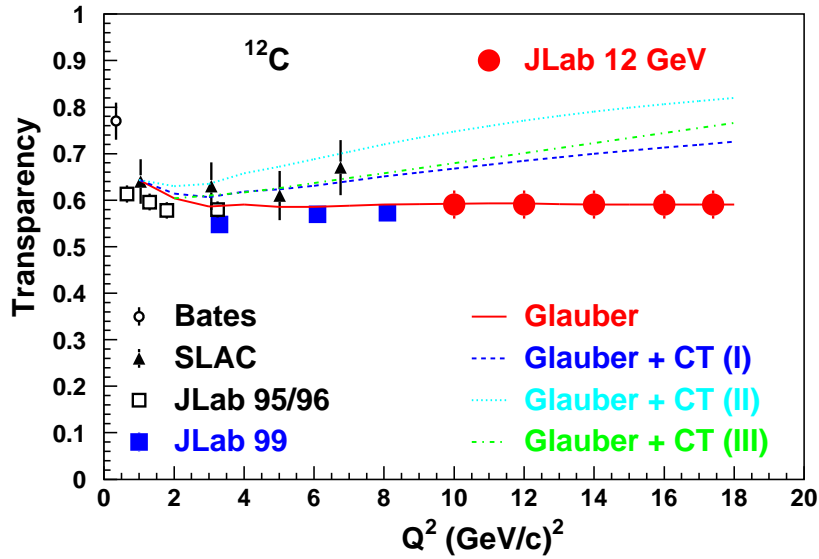


Figure 13. The Q^2 -dependence of T as defined in Eqn. (21). “Glauber” - calculation within Glauber approximation, “Glauber+CT(I) and Glauber+CT(II)” - calculations including CT effects with expansion parameter $\Delta M^2 = 1.1 \text{ GeV}^2$ and $\Delta M^2 = 0.7 \text{ GeV}^2$ respectively [150], “Glauber+CT(III)” - CT effects are included according to Ref. [151].

The recent Jefferson Lab data [149] allow us to put some constraints on the parameters defining the onset of CT. In Fig. 14 we analyze the lower limit of Q_0^2 at which PLCs are selected in γ^*N scattering. Since our interest is only in the energy dependence of the transparency, we normalized the calculations to the data at $Q^2 = 2 \text{ GeV}^2$ to avoid uncertainties related to the Q^2 dependence of quenching⁺ The analysis is done within the quantum diffusion model of CT for the range of the expansion parameter ΔM^2 ($\Delta M^2 = 0.7 \text{ GeV}^2$ in Fig. 14(a) and $\Delta M^2 = 1.1 \text{ GeV}^2$ in Fig.14(b)) consistent with the EVA data. In the case of the slower expansion rate, Fig. 14(a), the transparency is rather sensitive to Q_0^2 and the analysis yields a lower limit of $Q_0^2 \approx 6 \text{ GeV}^2$. For a faster expansion rate, Fig. 14(b), the nuclear transparency is less sensitive to Q_0^2 , since for intermediate range of Q^2 the PLC expands well before it escapes the nucleus. The analysis in Fig. 14(b) yields $Q_0^2 \geq 4 \text{ GeV}^2$. Combining these two analyses one can set the lower limit for the formation of PLCs at $Q_0^2 \approx 4 \text{ GeV}^2$ (see Eqn. (5) for implication of this limit in SRC studies).

The upgrade of Jefferson Lab would improve the situation, by pushing the measurement of T to a high enough Q^2 where the color transparency predictions appreciably diverge from the predictions of conventional calculations (see Figs. 13 and 14). Indeed, the EVA data have established in a model independent way that

⁺ The transparency is defined in Eqn 21 is inversely proportional to the nuclear quenching. Hence a decrease of the quenching effect with an increase of Q^2 may mask the CT effects at intermediate $Q^2 \leq 2 \text{ GeV}^2$.

at least for nucleon momenta ≥ 7.5 GeV/c, expansion effects are not large enough to mask the increase of the transparency. Hence measurements at $Q^2 \geq 14$ GeV², corresponding to comparable momenta of the ejectile nucleon, would unambiguously answer the question whether nucleon form factors at these Q^2 are dominated by small or large size configurations.

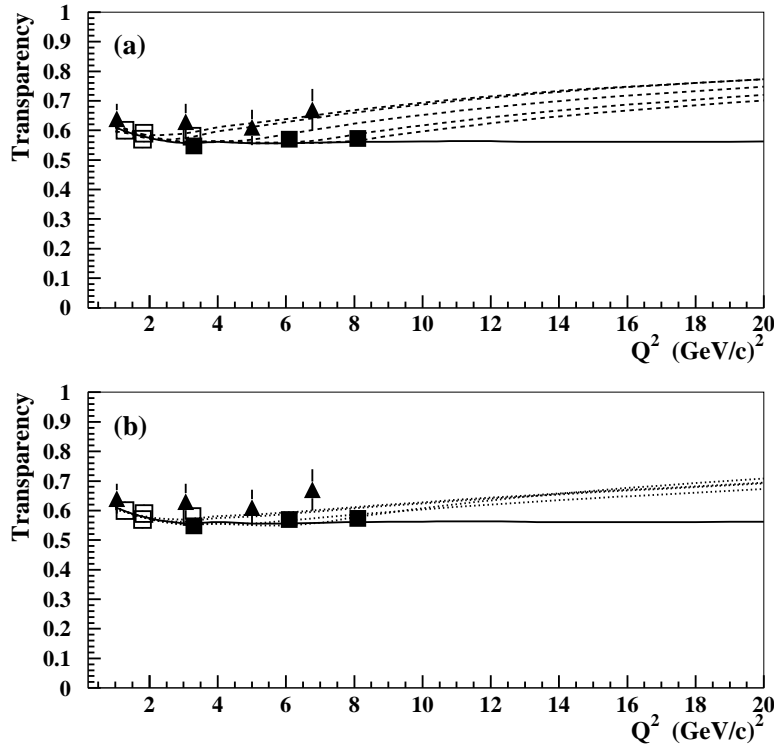


Figure 14. The Q^2 -dependence of T. The solid line is the prediction of the Glauber approximation. In (a) dashed curves correspond to the CT prediction with $\Delta M^2 = 0.7$ GeV² and with $Q_0^2 = 1$ (upper curve), 2, 4, 6 and 8 GeV²(lower curve). In (b) dotted curves correspond to the CT prediction with $\Delta M^2 = 1.1$ GeV² and with $Q_0^2 = 1$ (upper curve), 2, 4 and 6 GeV²(lower curve). All calculations are normalized to the data at $Q^2 = 2$ GeV². The data are the same as in Fig. 13.

Although $(e, e'N)$ measurements will allow an unambiguous check of the existence of color transparency, it will require a challengingly high accuracy from experiments to investigate the details of the expansion effects (Fig. 13). Thus, although this is the simplest reaction to measure, a much wider range of reactions would be necessary to build a sufficiently complete picture of phenomenon and to scan the expansion of the small size wave packets.

To obtain a more detailed knowledge of the interaction of PLCs with nuclei we can also select a processes in which the ejectile could interact a second time during its propagation through the nucleus [152, 153, 52] (double scattering reactions). This can be done by studying recoil nucleons with perpendicular (vs \vec{q}) momenta $p_{s,\perp} \geq 200$ MeV/c. At low Q^2 , the majority of such high momentum nucleons come from rescattering with

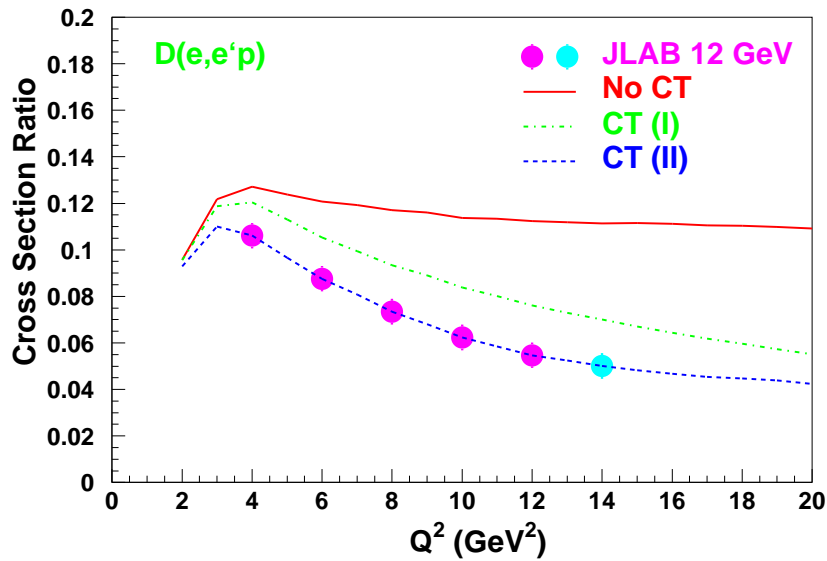


Figure 15. The ratio of the cross section at 400 MeV/c missing momentum to the cross section at 200 MeV/c as a function of Q^2 . Solid line corresponds to the GEA prediction. Dashed and dash-dotted lines represent the quantum diffusion model of CT with $\Delta M^2 = 0.7$ and 1.1 GeV² respectively. The drop with Q^2 in the color transparency models comes from a reduction in the rescattering of the struck nucleon, which is the dominant source of events with $P_m > k_F$.

the spectator nucleon in the nucleus. Therefore, the number of such nucleons should decrease substantially with the onset of CT which reduces the probability of rescattering. An important advantage of a double scattering reaction is that the disappearance of the final state interactions can be studied using the lightest nuclei (D, ³He, ⁴He), for which wave functions are known much better and where one can use a generalized eikonal approximation, which accounts for the nonzero values of the momenta of recoil nucleons [52, 31] *. Another advantage of double scattering reactions is that inter-nucleon distances probed are not large, 1 – 2 fm. These distances are comparable to the coherence length for values of Q^2 as low as about 4 – 6 GeV², and may provide evidence for a number of color coherent phenomena in the transitional Q^2 region. Ultimately, double scattering measurements will allow us to determine whether the lack of the CT in $A(e, e'p)$ reactions at $Q^2 \geq 8$ GeV² region is related to the large expansion rate of PLCs, or if it is because PLCs are not produced at all for these values of Q^2 .

An appropriate measure for color transparency in double scattering reactions is a ratio of cross sections, measured at kinematics for which double scattering is dominant, to the cross section measured at kinematics where the effect of Glauber screening is more important. Theoretical investigations of these reactions [153, 52] demonstrated that it is possible to separate these two kinematic regions by choosing two momentum intervals for the recoil nucleon: (300 – 500 MeV/c) for double scattering, and (0 – 200 MeV/c) for

* Note that in conventional Glauber approximation, the momenta of recoil nucleons are neglected.

Glauber screening. To enhance the effect of the final state interaction in both regions, the parameter α , characterizing the light cone momentum fraction of the nucleus carried by the recoiling nucleon should be close to one ($\alpha = (E_s - p_s^z)/m \approx 1$, where E_s and \mathbf{p}_s are the energy and momentum of recoil nucleon in the final state). Thus, the suggested experiment will measure the Q^2 -dependence of the following typical ratio at $\alpha = 1$:

$$R = \frac{\sigma(p_s = 400 \text{ MeV}/c)}{\sigma(p_s = 200 \text{ MeV}/c)} \quad (22)$$

Figure 15 shows this ratio, calculated within the generalized eikonal approximation (solid line), and using the quantum diffusion model of CT with upper and lower values of the expansion parameter ΔM^2 .

It is worth noting that in addition to the $d(e, e'pn)$ process, one can consider excitation of baryon resonances produced in the spectator kinematics, like $d(e, e'p)N^*$ and $d(e, e'N)\Delta$. The latter process is of special interest for looking for the effects of so-called chiral transparency—the disappearance of the pion field of the ejectile [154, 155].

3.4.1. Experimental Objectives The $A(e, e'p)$ and $d(e, e'p)$ experiments described in the previous Section are rather straightforward: they require a high-luminosity electron beam to access the very small cross sections at high- Q^2 and a set of two medium-resolution magnetic spectrometers to determine, with reasonable precision, the recoil nucleon's momentum and the nucleon's binding energy.

In the case of the $A(e, e'p)$ transparency measurements, the nuclear recoil momentum is typically restricted to a momentum smaller than the Fermi momentum k_F ($\approx 250\text{--}300 \text{ MeV}/c$). The missing energy (identical to the binding energy plus nuclear excitation energy) is restricted to be well below pion production threshold ($\approx 100 \text{ MeV}$). SRCs within a nuclear system push a sizable amount of the individual nucleons to large momenta and binding energies. As precise, quantitative evidence of this effect remains elusive, it is preferable to restrict oneself to the region of single particle strength described by above cuts in recoil nucleon momentum and missing energy.

Using two medium-resolution magnetic spectrometers, with momentum and angular resolutions of order 0.1% and 1 mr, one can easily make well-defined cuts in recoil nucleon momentum and missing energy. In the case of the $d(e, e'p)$ cross section ratio measurement, a good determination of the recoil nucleon's momentum is a fundamental concern: the recoil nucleon momentum distribution drops steeply with missing momentum, even though the double rescattering mechanism partly counteracts this effect. This is illustrated by the absolute value of the cross section ratio in Fig. 15, ≈ 0.1 , for recoil nucleon momenta of 400 MeV/c with respect to 200 MeV/c. Moreover, at 200 MeV/c the cross section varies with recoil nucleon momentum by about 30% per 10 MeV/c. Hence, an absolute comparison of the measured $d(e, e'p)$ cross section ratio with calculations requires determination of the recoil nucleon momentum value with precision much smaller than 10 MeV/c.

The use of large non-magnetic devices, such as electromagnetic calorimeters, may be possible in limited cases, but will seriously affect the required missing momentum

determination. Thus, for the $A(e, e'p)$ and $d(e, e'p)$ examples shown in Figs. 13 and 15, two magnetic spectrometers operating at a luminosity of 1×10^{38} electron-atoms/cm²/s, with 3 and 6 msr solid angle, respectively, were assumed. The larger solid angle magnetic spectrometer would detect the quasi-elastically scattered electrons, the smaller solid-angle would map the (relativistically boosted) Fermi cone. The latter magnetic spectrometer would need a momentum range between 4 GeV/c ($Q^2 \approx 6$ (GeV/c)²) and 10 GeV/c ($Q^2 \approx 17$ (GeV/c)²). Missing energy and recoil nucleon momentum resolutions would still be better than 10 MeV and 10 MeV/c, respectively.

Lastly, the estimated beam time for the projected uncertainties in Figs. 13 and 15 would be less than one month of beam time for the $^{12}\text{C}(e, e'p)$ transparency measurements, and one month of beam time for the $d(e, e'p)$ cross section ratio measurements up to $Q^2 = 12$ (GeV/c)², with one additional month required to push these ratio measurements to $Q^2 = 14$ (GeV/c)². For the cross section ratio measurements, one would need to determine the cross section yields at recoil nucleon's momenta of 200 and 400 MeV/s with two separate angle settings of the magnetic spectrometer (included in the estimated beam times). Note that the $d(e, e'p)$ measurements will build on the existing Jefferson Lab experiments[42, 43] at 6 GeV which plan to study the ratio R (Eq.(22)) up to Q^2 of 6 GeV².

3.5. Color Coherent Effects with Coherent Vector Meson Production off the Deuterium

Although the main emphasis in color transparency studies is given to the experiments with nucleon electroproduction, it is widely expected that one should observe the onset of color coherence in meson electroproduction at lower values of Q^2 than for the case of nucleon knockout. It should be easier to find the quark and anti-quark of a meson close together to form a point like configuration, than to find the three quarks of a nucleon together.

The QCD factorization theorem[119] for the exclusive meson production by the longitudinally polarized virtual photons demonstrates that the $q\bar{q}$ PLCs dominate in the Bjorken limit and that CT should occur both for the coherent and incoherent channels. In the leading twist the exclusive meson production can proceed through the quark-antiquark and, in case of vector mesons, also through the two gluon ladder exchange in t-channel[119]. At small x (probed for example at HERA[120]) the two gluon ladder exchange dominates in the production of ρ and ω -mesons. However at Jefferson Lab kinematics, production of ρ and ω -mesons is dominated by the quark exchange [119, 156]. The latter is confirmed by the analysis of HERMES data on $\gamma^* + p \rightarrow \rho + p$ reaction[156]. Additionally, the analyses of Ref. [156, 157, 158] indicate that the leading twist approximation overestimates strongly (by a factor ~ 4 for $Q^2 \sim 4$ GeV²) the ρ -meson production cross section. The suppression factor in leading approximation contribution is explained in Refs.[157, 156] as a higher twist effect due to the finite transverse size of the photon wave function in the convolution integral involving the interaction block, virtual photon, and meson wave functions. However,

the model analysis of [157] indicates that the higher twist effects may not interfere with the transverse localization of the vector meson wave function leading to a possibility of the sizable CT effects already at $Q^2 \geq 4 \text{ GeV}^2$. The suppression of the leading twist contribution was observed by [156] for the quark exchange channel for both vector meson and pion production. However the corresponding analysis of the transverse interquark distances is not yet available.

Studies of the CT for meson production with the Jefferson Lab upgrade will be very important for understanding of the onset of the leading twist contribution and determining what transverse separations are important in the higher twist contributions. An observation of CT for meson production would allow us to use these processes at pre-asymptotic Q^2 for measuring the ratios of different nucleon generalized parton distributions. In the case of the vector meson production it is feasible to look for CT both in coherent and incoherent scattering off nuclei [133, 22, 159, 118]. Studies of incoherent reactions require a very good energy resolution in the mass of the residual system to suppress processes where a meson is produced in the elementary reaction, processes like $\gamma_L + N \rightarrow M + \Delta$, as well as in a multi-step processes like $\gamma_L + N \rightarrow \rho + N, \rho + N^* \rightarrow \pi + N^{**}$. The first experiments looking for CT effects in the incoherent production of pions and ρ -mesons were recently approved at Jefferson Lab [160, 161].

Here we will focus on the reactions of the coherent meson production in which the background processes mentioned above are suppressed. The first experiment dedicated to the studies of coherent production of vector mesons from nuclei at 6 GeV approved recently at Jefferson Lab [162]. The proposed upgrade of Jefferson Lab, which will provide high energy, high intensity, and high duty factor beams makes systematic studies of these reactions a very promising area of study.

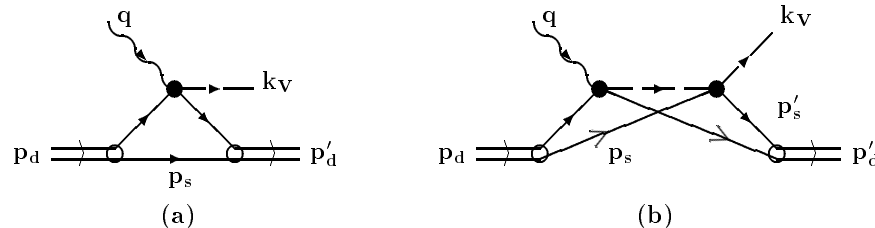


Figure 16. Diagrams corresponding to single (a) and double scattering contributions in coherent vector meson electroproduction.

The most promising channel for studying color coherent effects with meson electroproduction is the coherent production of vector mesons off deuteron targets:

$$e + d \rightarrow e' + V + d' \quad (23)$$

where “ V ” is the ρ , ω or ϕ meson. This reaction is a unique channel for studying CT for the following reasons:

- Due to the large *photon-vector meson* coupling the cross section of the process is large, and at high energies and small $Q^2 (< 1 \text{ GeV}^2)$ is well understood in the framework of the vector meson dominance (VMD) model;
- The deuteron is the theoretically best understood nucleus. It has zero isospin and as a result, in the coherent channel, $\rho - \omega$ mixing will be strongly suppressed, since the ρ and ω have isospin one and zero respectively. The technical advantage of using the deuteron in coherent reactions is the possibility of detecting the recoil deuterons.
- Coherent production of vector mesons off deuterium is characterized by two contributions: single and double scattering contributions (Fig. 16). Moreover, it is a well known fact from the photo-production experiments [163, 164] that at large $-t \geq 0.6 \text{ GeV}^2$, the double scattering contribution can be unambiguously isolated (Fig. 17).

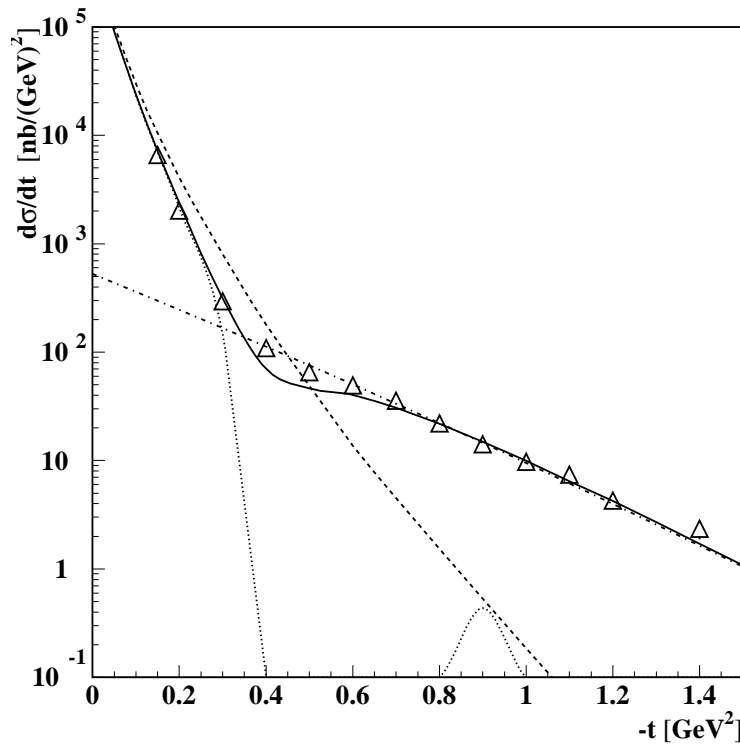


Figure 17. Cross section of the coherent ρ^0 photo-production off deuteron. Data are from [163, 164]. Dashed, dash-dotted, dotted and solid curves represent single scattering, double scattering, interference between single and double scattering, and full contributions respectively. Theoretical predictions are based on the vector meson dominance (VMD) model [167].

The strategy of CT studies in the coherent reaction of Eqn. (23) is somewhat similar to the strategies of studying CT in double scattering ($e, e'NN$) reactions. First one has to identify kinematics in which double scattering effects can be isolated from

Glauber type screening effects (corresponding to the interference term of single and double scattering amplitudes). The availability of the t -dependence of the differential cross section allows us to separate these kinematical regions. As Fig. 17 demonstrates, at $-t \leq 0.6 \text{ GeV}^2$ the cross section is sensitive to the screening effects, while at $-t \geq 0.6 \text{ GeV}^2$ it is sensitive to the double scattering contribution. Afterwards one has to study the Q^2 -dependence of the cross sections in these kinematic regions.

To identify unambiguously the observed Q^2 -dependence with the onset of CT one should however impose additional kinematic constraints based on the fact that in lepto-production processes, the longitudinal interaction length plays an important role and has a characteristic Q^2 -dependence (see e.g. [165]):

$$l_c = \frac{2\nu}{Q^2 + m_V^2 - t_{min}}. \quad (24)$$

An important aspect of the measurements is the ability to separate the effects of a changing longitudinal interaction length from those of color coherence with an increase of Q^2 . This can be achieved by keeping l_c fixed in a Q^2 scan of the coherent cross section at a wide range of momentum transfers t .

Based on the above discussions one can identify a CT observable as the ratio of two differential cross sections at fixed l_c but at different t : one in the double scattering (t_1), and another in the screening (t_2) regions,

$$R = \frac{d\sigma(Q^2, l_c, t_1)/dt}{d\sigma(Q^2, l_c, t_2)/dt} \quad (25)$$

Figure 18 presents model calculation of the Q^2 -dependence of ratio R for ρ production for $-t_1 = 0.8 \text{ (GeV/c)}^2$ and $-t_2 = 0.4 \text{ (GeV/c)}^2$. The upper curve is calculated without CT effect, within VMD with a finite longitudinal interaction length taken into account [166]. The lower band corresponds to calculations within the quantum diffusion model of CT [126] with different assumptions for CT [167] with respect to the expansion of the PLC and its interaction with the spectator nucleon. The upper and the lower limits in the band correspond to $\Delta M^2 = 1.1$ and 0.7 GeV^2 respectively (see discussion in Sec.(3.3)).

It is worth noting that for a complete understanding of the coherent production mechanism and the formation of the final mesonic states, these measurements should also be carried out at $Q^2 < 1 \text{ GeV}^2$ to allow us to match the theoretical calculations with VMD.

3.5.1. Experimental Objectives The experiment studying the reaction of Eqn. (23) will be the part of a broad effort to establish the existence of color transparency in QCD at intermediate energies. A large acceptance detector such as CLAS at Jefferson Lab is an ideal tool for conducting such experiments. With a single setting it can simultaneously measure the coherent production of all vector mesons in a broad kinematic range. Figure 19 shows the accessible kinematical range for an 11 GeV electron beam energy with CLAS++. The lines show the $Q^2 - W$ dependence at fixed coherent length l_c .

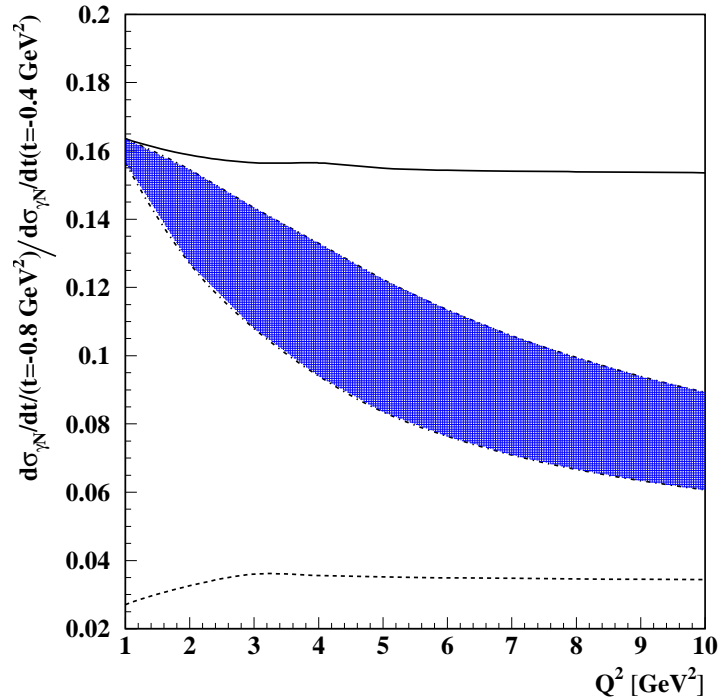


Figure 18. The ratio R of the cross sections at transferred momenta $-t = 0.4 \text{ GeV}/c^2$, and $-t = 0.8 \text{ GeV}/c^2$ as a function of Q^2 .

The plot shows that at this energy, the shape of the t -dependence can be studied up to $Q^2 = 5 \text{ (GeV}/c)^2$ at $l_c \sim 0.8$.

In the final state, the scattered electron and the recoil deuteron will be detected together with the decay products of the produced vector meson. In the case of $\rho^0 \rightarrow \pi^+\pi^-$, only one of the decay pions will be detected, and missing mass technique will be used to identify the second one. Additional suppression of the three pion final state ($\pi^+\pi^-\pi^0$) can be achieved by using a veto on a neutral hit in the CLAS calorimeters. For identification of the ω , a neutral hit in the calorimeters will be used to suppress the ρ^0 background. ϕ mesons will be identified via their K^+K^- decay, detecting one of the kaons. Count rates are estimated with acceptance calculations using CLAS++, assuming a luminosity $\mathcal{L} = 10^{35} \times A/Z \text{ cm}^{-2} \text{ sec}^{-1}$.

In Fig. 20, the expected errors on the ratio of cross sections of Eq. (25) is presented for the same kinematical conditions as in Fig. 18, with l_c fixed at 0.8 fm. The cross sections are calculated according to Ref. [167]. The statistical errors correspond to 30 days of beam time. This figure shows that the accuracy of the experiment will allow one to unambiguously verify the onset of CT in this region of Q^2 .

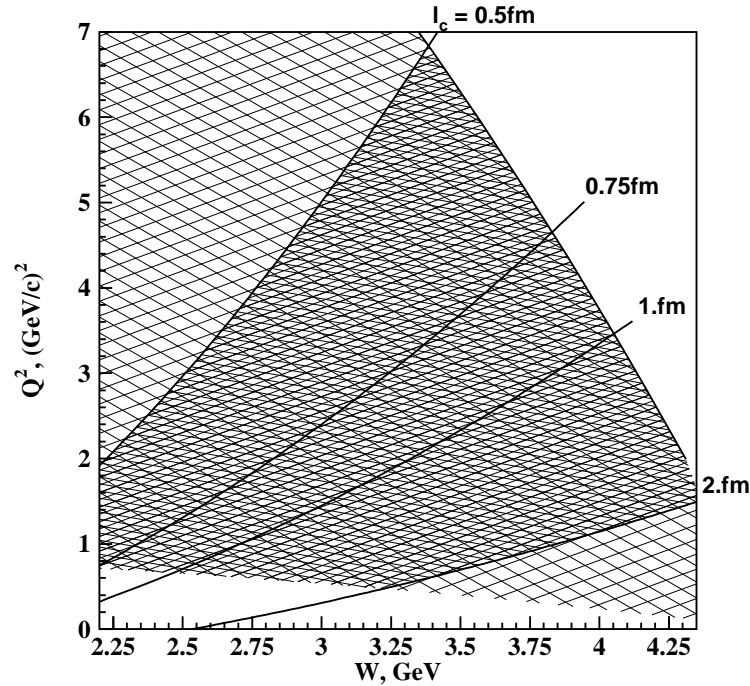


Figure 19. The accessible range of Q^2 and W at 11 GeV beam energy with new design of CLAS. Light shaded region is defined by the detection of the scattered electrons in the forward region of the CLAS. Dark shaded region is the preferred kinematical region for the proposed experiment. Lines represent $Q^2 - W$ dependence at a fixed longitudinal interaction length.

4. Summary and Discussion

Quantum Chromodynamics provokes a number of interesting questions related to nuclear physics. This review has addresses two of these:

- What is the quark nature of nuclei at low temperature and high density?
- What is the influence of color on hadron-nucleon interactions in nuclei?

Our central theme is that the use of Jefferson Laboratory, with electron energies up to 11 GeV, will lead to substantial progress in answering these questions.

New studies of deep inelastic scattering by nuclear targets will focus on the first question. We discuss how the search for scaling in deep inelastic scattering at values of Bjorken $x > 1$ will focus on a microscopic study of the nature of the quantum fluctuations which briefly transform ordinary nuclear matter into a high density system. Furthermore, the measurement of backward going nucleons in coincidence with the outgoing electron (denoted as tagging the structure function) will lead to disentangling the various models which have been proposed as explaining the nuclear EMC effect and thereby establish a clear signature of quark degrees of freedom in the nuclear structure

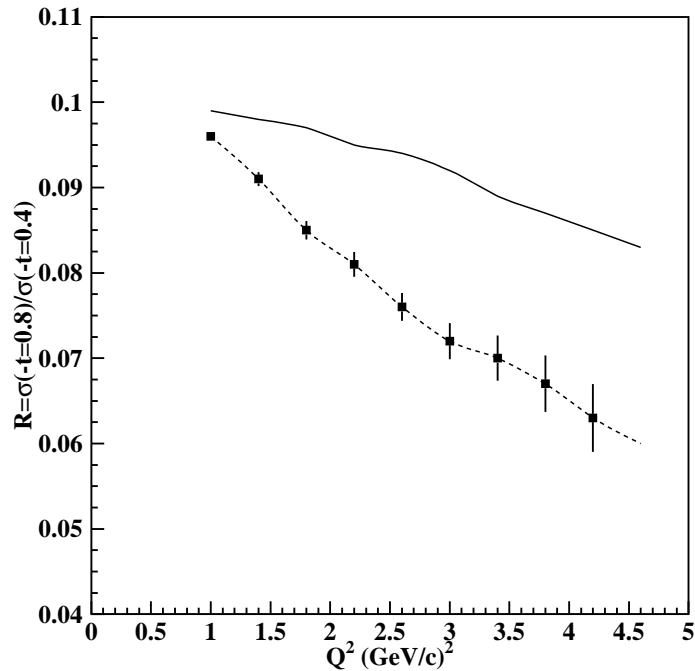


Figure 20. Expected errors on the ratio of cross sections at transferred momenta $0.4 \text{ GeV}/c^2$ and $0.8 \text{ GeV}/c^2$ for 2000 hours of running on CLAS with 11 GeV beam. The kinematics are fixed at $0.75 \leq l_c \leq 0.8$. The solid curve is the calculation of the ratio assuming no color transparency effects, the points are with color coherent effect. Events in each point are integrated in the bins of $\Delta Q^2 = 0.4 \text{ GeV}/c^2$ and $\Delta l_c = 0.2$. We assume a CLAS++ luminosity of $\mathcal{L} = 10^{35} \times A/Z \text{ cm}^{-2} \text{ sec}^{-1}$.

New studies of the knockout of one or two nucleons by electrons at high momentum transfer offer the promise of revealing how color influences the interaction between an ejected color singlet particle and the spectator nucleons. The absence of significant final state interactions, known as color transparency, would allow the discovery of a novel new phenomenon in baryon interactions. New measurements of the electroproduction of vector mesons in coherent interactions with a deuteron target will show how color influences meson-nucleon interactions.

The questions we discuss have been perplexing physicists for more than twenty years. The use of Jefferson Laboratory, with its well known high resolution, high duty factor, and high luminosity, at an energy of $\simeq 12 \text{ GeV}$, will finally provide the long desired answers.

Acknowledgments

This work is supported by DOE grants under contracts DE-FG02-01ER-41172, DE-FG02-96ER-40960, DE-FG02-96ER40950, DE-FG03-97ER-41014 and W-31-109-ENG-

38. This work was supported also by the Israel Science Foundation funded by the Israel Academy of Science and Humanities. We gratefully acknowledge also the support from Jefferson Lab. The Thomas Jefferson National Accelerator Facility (Jefferson Lab) is operated by the Southeastern Universities Research Association (SURA) under DOE contract DE-AC05-84ER-40150.

References

- [1] Drake J J *et al* 2002 *Astrophys. J.* **572** 996
- [2] Rock S *et al* 1982 *Phys. Rev. C* **26** 1592
- [3] Rock S *et al* 1992 *Phys. Rev. D* **46** 24
- [4] Day D *et al* 1979 *Phys. Rev. Lett.* **43** 1142
- [5] Day D *et al* 1987 *Phys. Rev. Lett.* **59** 427
- [6] Frankfurt L L, Strikman M I, Day D B, Sargsian M, 1993 *Phys. Rev. D* **48** 2451
- [7] Liuti S, 1993 *Phys. Rev. C* **47** R1854
- [8] Egiyan K Sh 2002 Study of Nucleon Short Range Correlations in $A(e, e')X$ reactions at $x_B > 1$
Proc. of the 9th International Conference on the Structure of Baryons
- [9] Pandharipande V R, Sick I and deWitt Huberts P K A 1997 *Rev. Mod. Phys.* **69** 981
- [10] Frankfurt L L and Strikman M I 1981 *Phys. Rept.* **76** 215
- [11] Arrington J *et al* 1999 *Phys. Rev. Lett.* **82** 2056
- [12] Arrington J, Day D B, Filippone W B and Lung A (spokespersons) 2002 Inclusive Scattering from Nuclei at $x > 1$ and High Q^2 with a 6 GeV Beam *Jefferson Lab Proposal E02-019*
- [13] Weinstein L B 2001 NN Correlations Measured in ${}^3\text{He}(e, e'pp)n$ *Proc. of Fifth Workshop on Electromagnetically Induced Two-Hadron Emission*
- [14] Cardman L *et al* (ed) 2001 The Science Driving the 12 GeV Upgrade of CEBAF *Jefferson Lab Report*
- [15] Aubert J J *et al* (European Muon Collaboration) 1983 *Phys. Lett. B* **123** 275
- [16] Bodek A *et al* 1983 *Phys. Rev. Lett.* **50** 1431
- [17] Bodek A *et al* 1983 *Phys. Rev. Lett.* **51** 534
- [18] Bickerstaff R P, Birse M C and Miller G A 1984 *Phys. Rev. Lett.* **53** 2532
- [19] Ericson M and Thomas A W 1984 *Phys. Lett. B* **148** 191
- [20] Berger E L 1986 *Nucl. Phys. B* **267** 231
- [21] Alde D M *et al* 1990 *Phys. Rev. Lett.* **64** 2479
- [22] Frankfurt L L and Strikman M I 1988 *Phys. Rept.* **160** 235
- [23] Frankfurt L L, Strikman M I and Liuti S 1990 *Phys. Rev. Lett.* **65** 1725
- [24] Gousset T and Pirner H J 1996 *Phys. Lett. B* **375** 349
- [25] Miller G A 1989 *Phys. Rev. C* **39** 1563
- [26] Brown G E and Rho M 1991 *Phys. Rev. Lett.* **66** 2720.
- [27] Alford M, Rajagopal K and Wilczek F 1998 *Phys. Lett. B* **422** 247
- [28] Carter G W and Diakonov D 2000 *Nucl. Phys. B* **582** 571
- [29] Rapp R, Schafer T, Shuryak E V and Velkovsky M 1998 *Phys. Rev. Lett.* **81** 53
- [30] Dieterich S *et al* 2002 to be submitted to *Phys. Rev. Lett.*
- [31] Frankfurt L L, Sargsian M M and Strikman M I 1997 *Phys. Rev. C* **56** 1124
- [32] Sargsian M M 2001 *Int. J. Mod. Phys. E* **10** 405
- [33] Feynman R 1972 *Photon-Hadron Interactions* (Reading: Benjamin)
- [34] Frankfurt L L, Kondratyuk A, and Strikman M I
- [35] Frankfurt L L, Miller G A, Sargsian M M and Strikman M I 2000 *Phys. Rev. Lett.* **84** 3045
- [36] Goggi G *et al* 1977 *Phys. Lett. B* **72** 265
- [37] Stoler P 1993 *Phys. Rept.* **226** 103

- [38] Arrington J 2002 Nucleon Momentum Distributions From a Modified Scaling Analysis of Inclusive $e - A$ Scattering *Proc. of the 9th International Conference on the Structure of Baryons*
- [39] Frankfurt L L and Strikman M I 1978 *Phys. Lett. B* **76**, 285
- [40] Frankfurt L L and Strikman M I 1983 *Nucl. Phys. A* **405** 557
- [41] Ulmer P and Jones M 1994 In-Plane Separations and High Momentum Structure in $d(e,e'p)n$ *Jefferson Lab Proposal E94-004*
- [42] Kuhn S E and Griffioen K A (spokespersons) 1994 Electron Scattering from a High Momentum Nucleon in Deuterium *Jefferson Lab Proposal E94-102*
- [43] Egiyan K Sh, Griffioen K A and Strikman M I (spokespersons) 1994 Measuring Nuclear Transparency in Double Rescattering Processes *Jefferson Lab Proposal E94-019*
- [44] Boeglin W, Jones M, Klein A, Mitchell, Ulmer P and Voutier E (spokespersons) 2001 Short-Distance Structure of the Deuteron and Reaction Dynamics in ${}^2\text{H}(e,e'p)n$ *Jefferson Lab Proposal E01-020*
- [45] Dutta D *et al* 2000 *Phys. Rev. C* **61** 061602
- [46] Liyanage N *et al* [Jefferson Lab Hall A Collaboration] *Phys. Rev. Lett.* 2001 **86** 5670
- [47] Lapikas L *et al* 2000 *Phys. Rev. C* **61** 064325
- [48] Frankfurt L, Strikman M and Zhalov M 2001 *Phys. Lett. B* **503** 73
- [49] Abbott D *et al* 1998 *Phys. Rev. Lett.* **80** 5072
- [50] BigBite Spectrometer <http://hallaweb.jlab.org/equipment/BigBite/index.html>
- [51] Piassetzky E, Bertozzi W, Watson J and Wood S (spokespersons) 2001 Studying the Internal Small-Distance Structure of Nuclei Via the Triple Coincidence (e,epN) Measurement *Jefferson Lab Proposal E01-015*
- [52] Frankfurt L L *et al* *Z. Phys. A* **352** 97
- [53] Friedman J I and Kendall H W 1972 *Ann. Rev. Nucl. Part. Sci.* **22** 203
- [54] Bjorken J D and Paschos E A 1969 *Phys. Rev.* **185** 1975
- [55] Benvenuti A C *et al* (BCDMS Collaboration) 1994 *Z. Phys. C* **63** 29
- [56] Vakili M *et al* (CCFR Collaboration) 2000 *Phys. Rev. D* **61** 052003
- [57] Arrington J *et al* 2001 *Phys. Rev. C* **64** 014602
- [58] Frankfurt L L, Day D B, Sargsian M M and Strikman M I 1993 *Phys. Rev. C* **48** 2451
- [59] Frankfurt L L, Sargsian M M and Strikman M I 1990 *Z. Phys. A* **335** 431
- [60] Frankfurt L L and Strikman M I 1985 *Nucl. Phys. B* **250** 1585
- [61] Frankfurt L L and Strikman M I 1980 *Phys. Lett. B* **94** 216
- [62] Lightbody J W and O'Connell J S 1988 *Computers in Physics* **May/June** 57
- [63] Benvenuti A C *et al* (BCDMS Collaboration) *Phys. Lett. B* **189** 483
- [64] Ashman J *et al* (EMC Collaboration) 1988 *Phys. Lett. B* **202** 603
- [65] Ashman J *et al* (EMC Collaboration) 1993 *Z. Phys. C* **57** 211
- [66] Dasu S *et al* 1994 *Phys. Rev. D* **49** 5641
- [67] Gomez J *et al* 1994 *Phys. Rev. D* **49** 4348
- [68] Arrington J (spokesperson) 2000 A Precise Measurement of the Nuclear Dependence of Structure Functions in Light Nuclei *Jefferson Lab Proposal E00-101*
- [69] Ciofi degli Atti C and Liuti S 1989 *Phys. Lett. B* **225** 215
- [70] Carlson C E, Lassila K E, and Sukhatme U P 1991 *Phys. Lett. B* **263** 377
- [71] Carlson C E and Lassila K E 1995 *Phys. Rev. C* **51** 364
- [72] Melnitchouk W, Sargsian M and Strikman M I 1997 *Z. Phys. A* **359** 359
- [73] Berge J P *et al* 1978 *Phys. Rev. D* **18** 1367
- [74] Efremenko V I *et al* 1980 *Phys. Rev. D* **22** 2581
- [75] Akulinichev S V, Kulagin S A and Vagrado G M 1985 *Phys. Lett. B* **158** 485
- [76] Kulagin S A 1989 *Nucl. Phys. A* **500** 653
- [77] Dunne G V and Thomas A W 1985 *Nucl. Phys. A* **446** 437c
- [78] Ericson M and Thomas A W 1983 *Phys. Lett. B* **128** 112
- [79] Friman B L, Pandharipande V R, and Wiringa R B 1983 *Phys. Rev. Lett.* **51** 763

- [80] Berger E L, Coester F and Wiringa R B 1984 *Phys. Rev. D* **29** 398
- [81] Jung H and Miller G A 1998 *Phys. Lett. B* **200** 351
- [82] Kaptari L P *et al* 1990 *Nucl. Phys. A* **512** 684
- [83] Melnitchouk W and Thomas A W 1993 *Phys. Rev. D* **47** 3783
- [84] Bickerstaff R P and Thomas A W 1989 *J. Phys. G: Nucl. Part. Phys.* **15** 1523
- [85] Miller G A and Smith J R 2002 *Phys. Rev. C* **65** 015211
- [86] Miller G A and Smith J R 2002 *Phys. Rev. C* **65** 055206
- [87] Hugenholtz N M and van Hove L 1958 *Physica* **24** 363
- [88] Koltun D S 1998 *Phys. Rev. C* **57** 1210
- [89] Melnitchouk W, Schreiber A W and Thomas A W 1994 *Phys. Rev. D* **49** 1183
- [90] Kulagin S A, Piller G and Weise W 1994 *Phys. Rev. C* **50** 1154
- [91] Gross, F and Liuti, S 1992 *Phys. Rev. C* **45** 1374
- [92] Guichon P A 1988 *Phys. Lett. B* **200** 235
- [93] Guichon P A M, Saito K, Rodionov E and Thomas A W 1996 *Nucl. Phys. A* **601** 349
- [94] Blunden P G and Miller G A 1996 *Phys. Rev. C* **54** 359
- [95] Close F E, Roberts R G and Ross G G 1983 *Phys. Lett. B* **129** 346
- [96] Jaffe R L, Close F E, Roberts R G and Ross G G 1984 *Phys. Lett. B* **134** 449
- [97] Close F E *et al* 1985 *Phys. Rev. D* **31** 1004
- [98] Nachtmann O and Pirner H J 1984 *Z. Phys. C* **21** 277
- [99] Güttner G and Pirner H J 1986 *Nucl. Phys. A* **457** 555
- [100] Frank M R, Jennings B K and Miller G A 1996 *Phys. Rev. C* **54** 920
- [101] Frankfurt L L and Strikman M I 1975 Proceedings of 10th Winter School of Physics on Nuclear Physics and Elementary Particle **2** 449
- [102] Brodsky S J and Chertok B T 1976 *Phys. Rev. D* **14** 3003
- [103] Matveev V A and Sorba P 1978 *Nuovo Cim. A* **45** 257
- [104] Pirner H J and Vary J P 1981 *Phys. Rev. Lett.* **46** 1376
- [105] Carlson C E and Havens T J 1983 *Phys. Rev. Lett.* **51** 261
- [106] Henley E M, Kisslinger L S and Miller G A 1983 *Phys. Rev. C* **28** 1277
- [107] Miller G A 1984 *Phys. Rev. Lett.* **53** 2008
- [108] Miller G A 1986 *Phys. Lett. B* **174** 229
- [109] Koch V and Miller G A 1985 *Phys. Rev. C* **31**
- [110] Mulders P J and Thomas A W 1984 *Phys. Rev. Lett.* **52** 1199
- [111] Mulders P J and Thomas A W 1983 *J. Phys. G* **9** 1159
- [112] Miller G A 1985 *Nucl. Phys. A* **446** 445.
- [113] Kondratyuk L A Shmatikov M 1985 *Sov. J. Nucl. Phys.* **41** 141
- [114] Lassila K E and Sukhatne U P 1988 *Phys. Lett. B* **209** 343
- [115] Chew G F and Low F E 1959 *Phys. Rev.* **113** 1640
- [116] Frankfurt L, Sargsian M and Strikman, *in preparation*
- [117] Frankfurt L, Miller G A and Strikman M 1993 *Phys. Lett. B* **304** 1
- [118] Brodsky S J, Frankfurt L, Gunion J F, Mueller A H and Strikman M 1994 *Phys. Rev. D* **50** 3134
- [119] Collins J C, Frankfurt L and Strikman M 1997 *Phys. Rev. D* **56** 2982
- [120] Abramowicz H and Caldwell A 1999 *Rev. Mod. Phys.* **71** 1275
- [121] Aitala E M *et al* (E791 Collaboration) 2001 *Phys. Rev. Lett.* **86** 4768
- [122] Aitala E M *et al* (E791 Collaboration) 2001 *Phys. Rev. Lett.* **86** 4773
- [123] Adams M R *et al* (E665 Collaboration) 1995 *Phys. Rev. Lett.* **74** 1525
- [124] Brodsky S J 1982 *Proc. of the Thirteenth Int'l Symposium on Multiparticle Dynamics* (Singapore: World Scientific) p 963
- [125] Mueller A H 1982 *Proc. of the Seventeenth Rencontres de Moriond* vol 1 (Gif-sur-Yvette: Editions Frontières) p 13
- [126] Farrar G R, Liu H, Frankfurt L L and Strikman M I 1988 *Phys. Rev. Lett.* **61** 686
- [127] Frankfurt L L, Strikman M and Zhalov M 1990 *Nucl. Phys. A* **515** 599

- [128] Jennings B K and Miller G A 1990 *Phys. Lett. B* **236** 209
- [129] Jennings B K and Miller G A 1991 *Phys. Rev. D* **44** 692
- [130] Jennings B K and Miller G A 1992 *Phys. Rev. Lett.* **69** 3619
- [131] Jennings B K and Miller G A 1992 *Phys. Lett. B* **274** 442
- [132] Bianconi A, Boffi S and Kharzeev D E 1993 *Phys. Lett. B* **305** 1
- [133] Brodsky S J and Mueller A H 1988 *Phys. Lett. B* **206** 685
- [134] Dokshitzer Y L, Khoze V A, Mueller A H and Troyan S I 1991 *Basics of Perturbative QCD* (Gif-sur-Yvette: Editions Frontières)
- [135] Frankfurt L L, Greenberg W R, Miller G A and Strikman M 1992 *Phys. Rev. C* **46** 2547
- [136] Szczepaniak A, Radyushkin A and Ji C 1998 *Phys. Rev. D* **57** 2813
- [137] Melic B, Nizic B and Passek K 1999 *Phys. Rev. D* **60** 074004
- [138] Frankfurt L, Miller G A and Strikman M 1993 *Nucl. Phys. A* **555** 752
- [139] Ralston J P and Pire B 1988 *Phys. Rev. Lett.* **61** 1823
- [140] Brodsky S J and de Teramond G F 1988 *Phys. Rev. Lett.* **60** 1924
- [141] Jain P, Pire B and Ralston J P 1996 *Phys. Rept.* **271** 67
- [142] Carroll A S *et al* 1988 *Phys. Rev. Lett.* **61** 1698
- [143] Frankfurt L L, Strikman M and Zhalov M 1994 *Phys. Rev.* **C50** 2189
- [144] Mardor Y *et al* 1998 *Phys. Rev. Lett.* **81** 5085
- [145] Leksanov A *et al* 2001 *Phys. Rev. Lett.* **87** 212301
- [146] Jennings B K and Miller G A 1993 *Phys. Lett. B* **318** 7
- [147] O'Neill T G *et al* 1995 *Phys. Lett. B* **B351** 87
- [148] Makins N C R *et al* *Phys. Rev. Lett.* **72** 1986
- [149] Garrow K *et al* 2001 *Preprint hep-ex/0109027, Phys. Rev. C in press*
- [150] Frankfurt L L, Moniz E J, Sargsian M M, Strikman M I 1995 *Phys. Rev. C* **51** 3435
- [151] Nikolaev N N, Szczurek A, Speth J, Wambach J, Zakharov B G and Zoller V R 1994 *Phys. Rev. C* **50** 1296
- [152] Frankfurt L L and Strikman M 1991 *Prog. in Part. and Nucl. Phys.* **27** 135
- [153] Egiyan K S *et al* *Nucl. Phys. A* **580** 365
- [154] Frankfurt L L, Miller G A and Strikman M 1994 *Ann. Rev. of Nucl. and Part. Sci.* **44** 501
- [155] Frankfurt L L, Lee T S H, Miller G A and Strikman M 1997 *Phys. Rev. C* **55** 909
- [156] Vanderhaeghen M, Guichon P A and Guidal M 1999 *Phys. Rev. D* **60** 094017
- [157] Frankfurt L, Koepf W, and Strikman M 1996 *Phys. Rev. D* **54** 3194
- [158] Mankiewicz L, Piller G and Weigl T 1998 *Eur. J. Phys.* **5** 119
- [159] Kopeliovich B Z, Nemchick J, Nikolaev N N and Zakharov B G 1993 *Phys. Lett. B* **309** 179
- [160] Ent R, Garrow K (spokespersons) 2001 Measurement of Pion Transparency in Nuclei *Jefferson Lab Proposal E01-107*
- [161] Hafidi K, Holtrop M, Mustapha B (spokespersons) 2002 Q^2 -dependence of Nuclear Transparency for Incoherent ρ^0 Production *Jefferson Lab Proposal E02-110*
- [162] Stepanyan S, Kramer L and Klein F (spokespersons) 2001 Coherent Vector Meson Production of Deuteron *Jefferson Lab Proposal E02-012*
- [163] Anderson R L *et al* 1971 *Phys. Rev. D* **4** 3245
- [164] Overman I D 1971 PhD. Thesis, SLAC-140, UC-34
- [165] Gribov V N 1970 *Sov. Phys.-JETP* **30** 709
- [166] Frankfurt L *et al* 1997 *Nucl. Phys. A* **622** 511
- [167] Frankfurt L, Piller G, Sargsian M and Strikman M 1998 *Eur. J. Phys. A* **2** 301